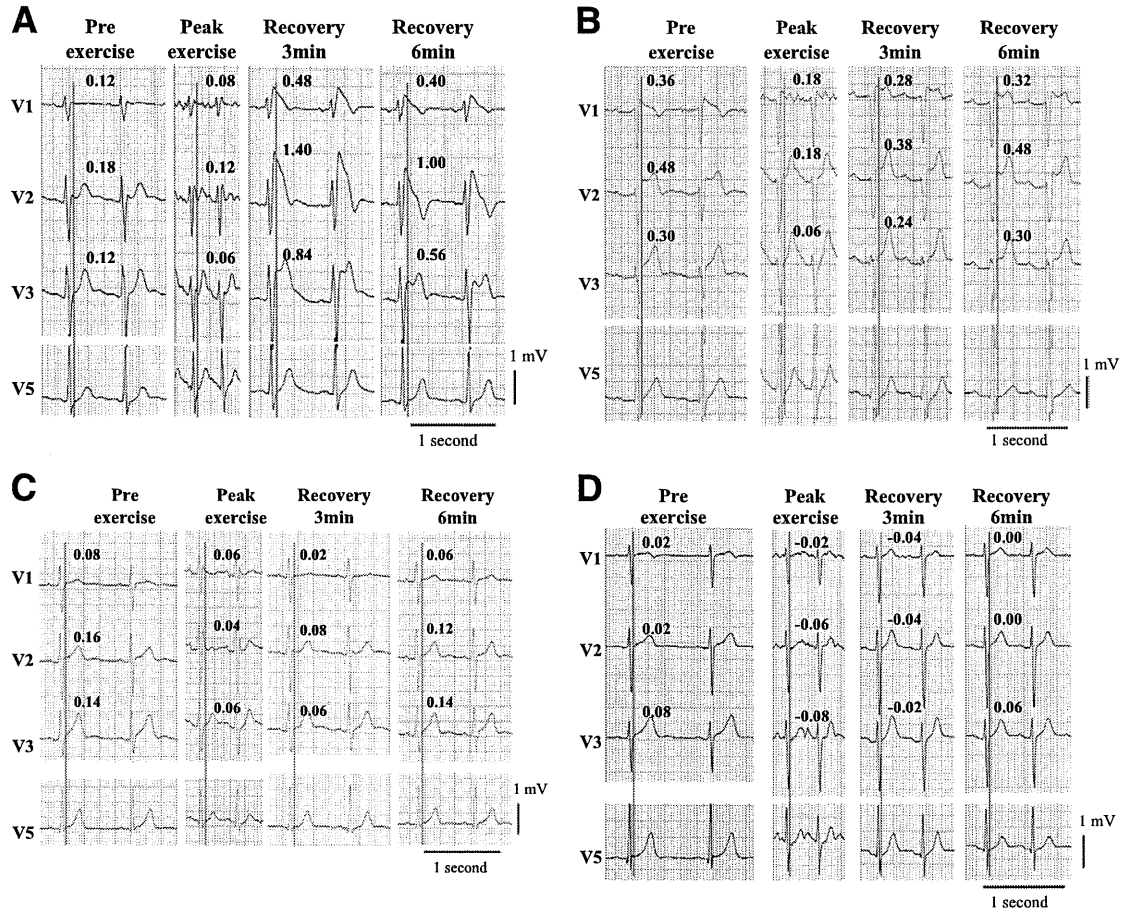

Figure 1 **Typical Responses of ST-Segment Amplitude in Leads V_1, V_2, V_3, and V_5 During Exercise Testing in Brugada Syndrome Patients**

(A) In the group 1 Brugada patient showing saddle-back type ST-segment (lead V_2) at baseline, ST-segment amplitude slightly decreased at peak exercise, but rea-scended at early recovery (3 min), resulting in typical coved-type ST-segment elevation. **(B, C)** In the group 2 Brugada patient and **(D)** in the control subject, ST-segment amplitude decreased at peak exercise and gradually recovered to the baseline at recovery. It is noteworthy that the peak J-point amplitude in lead V_2 was augmented despite not showing ST-segment augmentation in **A** and **C**. The ST-segment amplitudes are shown as numeric values expressed in millivolts (mV). The **red vertical line** indicates the line from the end point of the QRS interval at electrocardiography lead V_5.

amplitude and ST40 amplitude decreased in most patients of both groups.

Comparison of HRR is shown in Figure 3. The HRR of group 1 patients was significantly larger than that of group 2 patients (32 ± 15 vs. 23 ± 10, p = 0.0007) and control subjects (32 ± 15 vs. 26 ± 10, p = 0.021). The differences of HRR between group 2 patients and control subjects were also statistically significant (23 ± 10 vs. 26 ± 10, p = 0.026).

Although there were no sustained or nonsustained ventricular arrhythmias throughout exercise testing, single premature ventricular complexes were observed during exercise in 8 of the group 1 patients and in 11 of the group 2 patients, and at recovery in 10 of the group 1 patients and in 9 of the group 2 patients. There were no significant differences between groups 1 and 2 in incidences of premature ventricular complexes.

Clinical, laboratory, electrocardiographic, and electrophysiologic characteristics. Comparison of the clinical, laboratory, electrocardiographic, and electrophysiologic characteristics between groups 1 and 2 patients are shown in Table 2. There were no significant differences in these characteristics between groups 1 and 2 except for the presence of *SCN5A* mutation and late potential (*SCN5A* mutation, 17% vs. 5%, p = 0.048; late potential, 82% vs. 53%, p = 0.004).

Follow-up. The mean follow-up period for the 93 BrS patients was 75.7 ± 38.4 months. During follow-up, 25 of all 93 BrS patients (27%) had cardiac events, and the incidence of cardiac events was significantly higher in group 1 than in group 2 patients (44% vs. 17%, p = 0.004). The period from exercise testing to cardiac events ranged from 1 to 78 months (median 12 months). One patient in group 2, who refused implantation of ICD and was taking disopyr-

JACC Vol. 56, No. 19, 2010
November 2, 2010:1576–84

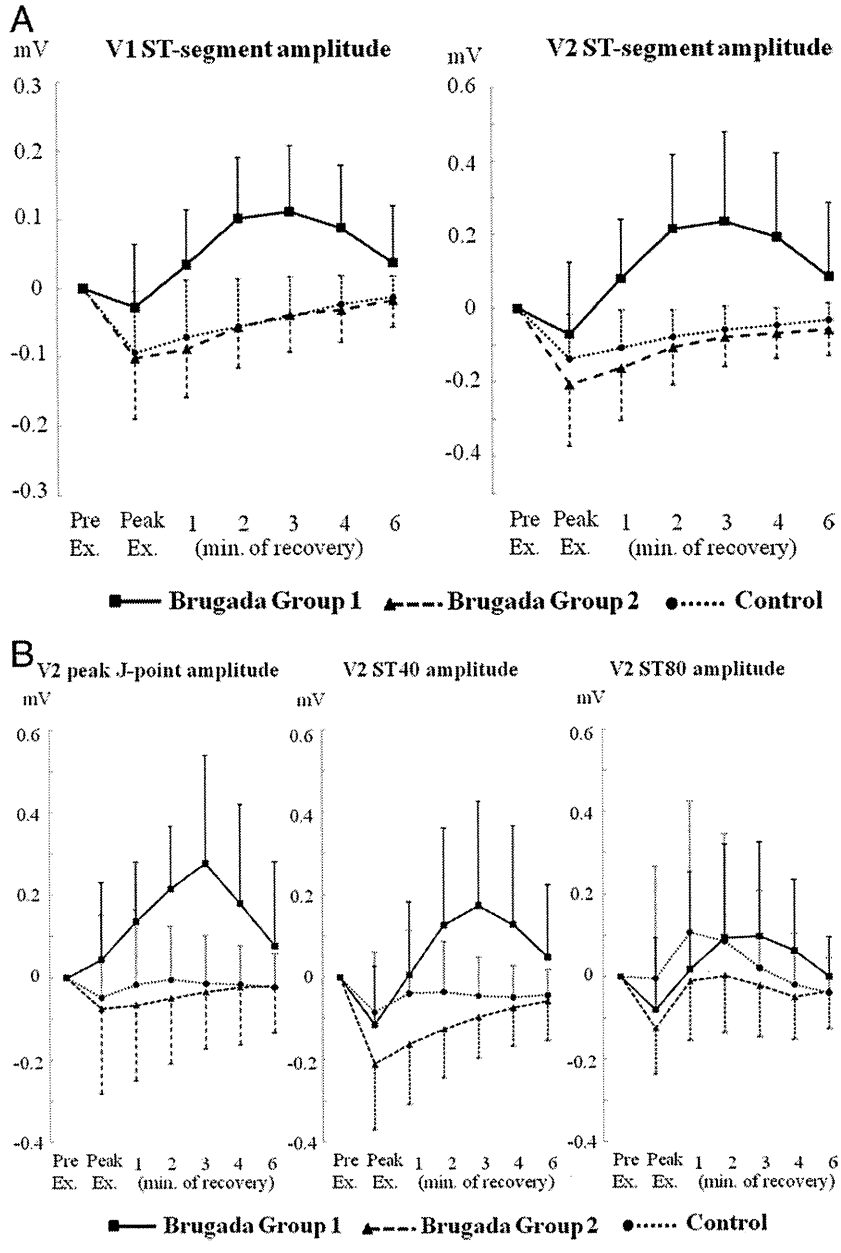

Figure 2 Composite Data of Serial Changes of ST-Segment Amplitude

(A) Composite data of serial changes of ST-segment amplitude in lead V_1 **(left)** and lead V_2 **(right)** during exercise (Ex.) testing in group 1 Brugada syndrome patients **(squares)** and group 2 Brugada syndrome patients **(triangles)**, and in control subjects **(circles)**. **(B)** Peak J-point amplitude **(left)**, ST40 amplitude **(middle)**, and ST80 amplitude **(right)** in lead V_2. The ST-segment amplitude decreased at peak exercise and started to reascend at early recovery, and culminated at 3 min of recovery in group 1 Brugada patients. In the group 2 Brugada patients and control subjects, the ST-segment amplitude decreased at peak exercise and gradually recovered to the baseline level during recovery. The peak J-point amplitude and ST40 amplitude during recovery showed the same trend as the ST-segment amplitude. Since ST80 amplitude was influenced by T wave, especially at rapid heart rate, the trends of the 3 groups were somewhat different from ST-segment amplitude or ST40 amplitude. The ST-segment amplitudes are shown as values compared to pre-exercise ST-segment amplitudes. $p < 0.05$.

amide 300 mg daily, died of VF. Three of 7 patients with medication had cardiac events, including 1 death.

Predictors of outcome. Kaplan-Meier analysis demonstrated significant differences in the time to the first cardiac event depending on the presence of ST-segment augmentation during recovery from exercise (Fig. 4A). Group 1 patients had a significantly higher cardiac event rate than group 2 patients (log-rank, $p = 0.0029$). Previous history of VF (Fig. 4B) and positive *SCN5A* mutation (Fig. 4C) also had significant values for occurrence of subsequent cardiac events ($p = 0.0013$ and $p = 0.028$, respectively); however, spontaneous coved-type ST-segment elevation did not predict cardiac events ($p =$

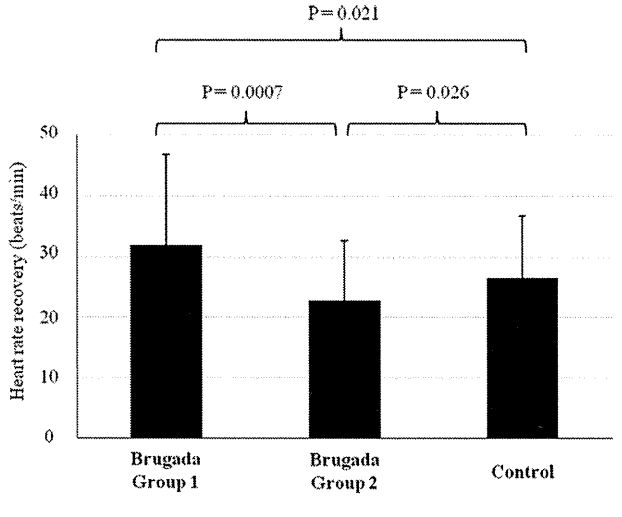

Figure 3 **Comparison of HRR After Exercise Cessation**

Comparison of heart rate recovery (HRR) 1 min after exercise cessation among Brugada syndrome patients of groups 1 and 2 and control subjects. The HRR in group 1 patients was significantly larger than that in group 2 (32 ± 15 beats/min vs. 23 ± 10 beats/min, p = 0.0007) and in control subjects (32 ± 15 beats/min vs. 26 ± 10 beats/min, p = 0.021). The differences of HRR between group 2 patients and control subjects were also significant (23 ± 10 beats/min vs. 26 ± 10 beats/min, p = 0.026).

0.068) (Fig. 4D). The results of Cox regression analysis are shown in Table 3. In univariate analysis, indexes predictive of cardiac events were previous episodes of VF (p = 0.003), ST-segment augmentation at early recovery (group 1; p = 0.005), and presence of *SCN5A* mutation (p = 0.037). In multivariate Cox regression analysis, previous episodes of VF and ST-segment augmentation at early recovery were significant and independent predictors of subsequent cardiac events (p = 0.005 and p = 0.007, respectively).

The incidence of cardiac events during follow-up in the subgroups according to symptoms before exercise testing is shown in Table 4. In the subgroup of 35 BrS patients with syncope alone, group 1 had a significantly higher cardiac event rate than group 2 (log-rank, 6 of 12 [50%] vs. 3 of 23 [13%], p = 0.016). Of note, among 36 asymptomatic patients, only 3 patients (9%) in group 1 experienced cardiac events. The log-rank test also demonstrated higher cardiac event risk in group 1 compared with group 2 (3 of 15 [20%] vs. 0 of 21 [0%], p = 0.039).

Discussion

The major findings of the present study were the following: 1) 37% of BrS patients showed ST-segment augmentation at early recovery during exercise testing; 2) ST-segment augmentation at early recovery was specific in BrS patients, and was significantly associated with a higher cardiac event rate, notably for patients with previous episode of syncope or for asymptomatic patients; and 3) BrS patients with ST-segment augmentation at early recovery showed significantly larger HRR. This is the first systematic report on the relationship between ST-segment augmentation during recovery from exercise and prognosis for BrS patients.

Augmentation of ST-segment elevation and possible mechanism. It is well known that autonomic function influences an extent of ST-segment elevation in BrS (8). The ST-segment elevation is mitigated by administration of β-adrenergic agonists and is enhanced by parasympathetic agonists such as acetylcholine in experimental and clinical investigations (5,14–16). Parasympathetic reactivation is thought to occur at early recovery after treadmill exercise testing, especially in the first minute after cessation of exercise (10,17). In the present study, we measured the ST-segment amplitude as a repolarization parameter rather than a depolarization parameter, and evaluated HRR to investigate the correlation between ST-segment augmentation and parasympathetic activity (9,18). The BrS patients who had ST-segment augmentation had significantly larger HRR compared with patients who did not, suggesting that the ST-segment augmentation was closely related to higher parasympathetic activity. However, it is still unclear whether ST-segment augmentation observed in the 34 BrS patients was simply due to more increased parasympathetic activity or to more increased susceptibility (hypersensitivity) to the parasympathetic reactivation.

Conversely, the *SCN5A* mutation was more frequently identified in group 1. Scornik et al. (19) reported that *SCN5A* mutation can accentuate parasympathetic activity toward the heart directly. It was also reported that specific mutations in the *SCN5A* gene may lead to augmentation of J-point amplitude or ST-segment amplitude during beta-adrenergic stimulation (20,21). Veldkamp et al. (20) demonstrated that a specific *SCN5A* mutation, 1795insD, augments slow inactivation, and delays recovery of sodium channel availability, thus reducing the sodium current and resulting in augmented peak J-point amplitude at rapid heart rate. Increased body temperature induced by exercise can be a risk of life-threatening arrhythmias in patients with BrS (22). A specific *SCN5A* missense mutation, T1620M, was reported to cause a faster decay of the sodium channel but slower recovery from inactivation, resulting in increased ST-segment elevation in precordial leads at higher temperatures during exercise. Although Amin et al. (13) reported that exercise induced augmentation of peak J-point amplitude, a depolarization parameter or at least combined parameter of both depolarization and repolarization, in all subjects tested, the incidence of increase in the peak J-point amplitude at peak exercise was lower (37%) in our Brugada patients. This is probably in part because only 9 (10%) of our 93 BrS patients had the *SCN5A* mutation. We could not identify significant differences in HRR, QRS duration, peak J-point amplitude (lead V_2), and ST-segment amplitude (leads V_1, V_2, V_3) at peak exercise between patients with and without *SCN5A* mutation (not shown), and that may be also due to the small number of BrS patients with *SCN5A* mutation.

Risk stratification in BrS. Implantation of an ICD is a first line of therapy for secondary prevention in patients with BrS who exhibited previous history of VF. The American College

JACC Vol. 56, No. 19, 2010
November 2, 2010:1576–84

Table 2 Clinical, Laboratory, Electrocardiographic, and Electrophysiologic Characteristics and Long-Term Follow-Up of Groups 1 and 2 Brugada Syndrome Patients

Characteristic	Group 1 (n = 34)	Group 2 (n = 59)	p Value
Clinical characteristics			
Age at exercise testing, yrs	42 ± 11	48 ± 15	NS
Men	34 (100%)	57 (97%)	NS
Family history of SCD at age <45 yrs or Brugada syndrome	7 (21%)	16 (27%)	NS
Documented AF	7 (21%)	12 (20%)	NS
Documented VF before exercise testing	7 (21%)	15 (25%)	NS
Syncope alone before exercise testing	12 (35%)	23 (39%)	NS
Asymptomatic before exercise testing	15 (44%)	21 (36%)	NS
Age at first cardiac event, yrs	42 ± 13	45 ± 15	NS
ICD implantation	25 (74%)	38 (64%)	NS
Laboratory characteristics			
SCN5A mutation	6 (17%)	3 (5%)	0.048
Electrocardiographic characteristics			
RR, ms	951 ± 170	953 ± 140	NS
PR, ms	184 ± 28	175 ± 31	NS
QRS, ms	98 ± 14	98 ± 17	NS
QTc, ms	418 ± 46	415 ± 43	NS
ST-segment amplitude (mV) at baseline			
V_1	0.14 ± 0.09	0.16 ± 0.12	NS
V_2	0.41 ± 0.22	0.38 ± 0.26	NS
V_3	0.22 ± 0.13	0.19 ± 0.14	NS
Spontaneous coved-type ST-segment elevation in right precordial leads	30 (88%)	43 (73%)	NS
Signal-averaged electrocardiogram			
TfQRS, ms	122 ± 15	118 ± 17	NS
Late potential	28/34 (82%)	30/57 (53%)	0.004
Premature ventricular complexes during exercise	8 (24%)	11 (19%)	NS
Premature ventricular complexes at recovery	10 (29%)	9 (15%)	NS
Electrophysiologic characteristics			
AH interval, ms	107 ± 24	98 ± 27	NS
HV interval, ms	45 ± 8	44 ± 11	NS
Induction of VF	26/31 (84%)	33/47 (70%)	NS
Follow-up			
Cardiac events	15 (44%)	10 (17%)	0.004
Follow-up period, months	74.1 ± 42.2	76.5 ± 36.4	NS

AF = atrial fibrillation; ICD = implantable cardioverter-defibrillator; SCD = sudden cardiac death; TfQRS = total filtered QRS duration; VF = ventricular fibrillation; other abbreviations as in Table 1.

of Cardiology/American Heart Association/Heart Rhythm Society guidelines refer to BrS patients who have had syncope as having Class IIa indication for ICD therapy (23). However, there is still much room for argument with respect to treatments for patients who have had only syncope, and for asymptomatic patients (24–28). Although inducibility of VF during EPS (25,26), family history of SCD (24), spontaneous type 1 ECG (25,27), and late potential (28) have been proposed as predictors of cardiac events, the availability of these indexes remains controversial (7,29).

In the present study, a previous episode of VF (or aborted cardiac arrest) was the strongest predictor of subsequent cardiac events, as in previous studies (7,30,31). Moreover, ST-segment augmentation at early recovery during exercise testing was a significant and independent predictor of subsequent cardiac events in the present study. The results suggested that parasympathetic activity plays an important role in both ST-segment augmentation and subsequent cardiac events. As previously noted, it remains unclear that the cause of ST-segment augmentation in our 34 patients was a result of more increased parasympathetic activity or of more increased susceptibility of the patients to the increased parasympathetic reactivation.

Study limitations. First, BrS patients were confined to those who were hospitalized in our hospital for close investigation. That indicates these patients can be biased toward relatively high risk. Second, the present study is based on data from a small population of 93 patients; hence, it was not sufficient to evaluate the prognosis, and there also was a small number of events. Although we adopted a step-wise approach, the limited number of events can lessen the precision of the consequences for multivariate Cox regression analysis.

Conclusions

The presence of *SCN5A* mutation was a significant predictor of subsequent cardiac events by univariate Cox regression analysis. However, multivariate Cox regression analysis showed it was not a significant predictor of prognosis.

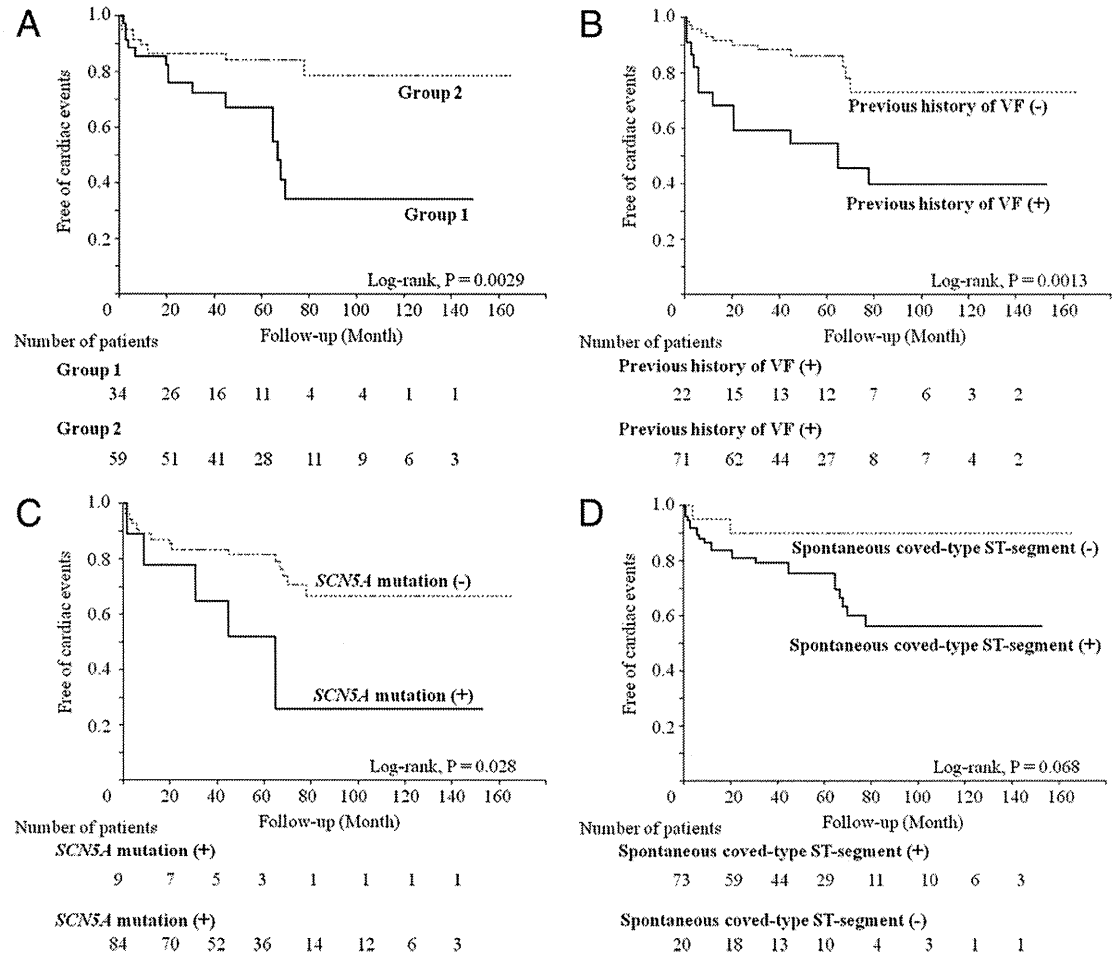

Figure 4 **Kaplan-Meier Analysis of Cardiac Events During Follow-Up**

Kaplan-Meier analysis of **(A)** cardiac events during follow-up, depending on patterns in response to ST-segment elevation during exercise test (groups 1 and 2), **(B)** incidence of previous episode of ventricular fibrillation (VF), **(C)** *SCN5A* mutation, and **(D)** spontaneous coved-type ST-segment elevation. Group 1 Brugada patients had a significantly higher cardiac event rate than did group 2 Brugada patients (log-rank, p = 0.0029). Brugada patients with previous episodes of VF or with *SCN5A* mutation had significantly greater values for occurrence of subsequent cardiac events than did patients without VF episodes or *SCN5A* mutation (p = 0.0013, p = 0.028, respectively), whereas spontaneous coved-type ST-segment elevation in Brugada patients did not predict cardiac events compared with patients not having such ST-segment elevation (p = 0.068).

Further study with a larger number of BrS patients will be required to evaluate the significance of the index as a predictor of subsequent cardiac events.

As for BrS patients with only syncope, subsequent cardiac events occurred in 50% (6 of 12) patients who exhibited ST-segment augmentation at early recovery. Asymptomatic

Table 3 **Predictive Capabilities of Cardiac Events**

		Univariate Analysis		Multivariate Analysis	
	Positive, n (%)	HR (95% CI)	p Value	HR (95% CI)	p Value
Previous episodes of VF	22 (24%)	3.40 (1.54–7.53)	0.003	3.25 (1.43–7.37)	0.005
Augmentation of ST-segment elevation at early recovery phase	34 (37%)	3.17 (1.42–7.09)	0.005	3.17 (1.37–7.33)	0.007
SCN5A mutation	9 (10%)	2.86 (1.07–7.66)	0.037		
Spontaneous coved-type ST-segment	72 (77%)	3.51 (0.83–14.9)	0.089		
Late potential	58/91 (64%)	2.25 (0.84–5.99)	0.11		
VF inducible in EPS	59/78 (76%)	0.73 (0.30–1.75)	0.48		
Family history of SCD or BrS	23 (25%)	1.19 (0.47–3.02)	0.72		

BrS = Brugada syndrome; CI = confidence interval; EPS = electrophysiologic study; HR = hazard ratio; other abbreviations as in Table 2.

JACC Vol. 56, No. 19, 2010
November 2, 2010:1576–84

Table 4 Incidence of Cardiac Events According to Symptoms Before Exercise Testing

Type	n	Treadmill Exercise Test	n	VF Occurrence	p Value (vs. Group 1)
Documented VF	22	Group 1	7	6 (86%)	
		Group 2	15	7 (47%)	0.14
Syncope alone	35	Group 1	12	6 (50%)	
		Group 2	23	3 (13%)	0.016
Asymptomatic	36	Group 1	15	3 (20%)	
		Group 2	21	0 (0%)	0.039

The p value was calculated according to the log-rank test.
VF = ventricular fibrillation.

patients who had ST-segment augmentation at early recovery had a higher incidence of cardiac events than patients who did not. These data suggested the potential utility of exercise testing to predict cardiac events for patients with BrS who have had previous episodes of only syncope but not VF or who have had no symptoms.

Reprint requests and correspondence: Dr. Wataru Shimizu, Division of Arrhythmia and Electrophysiology, Department of Cardiovascular Medicine, National Cerebral and Cardiovascular Center, 5-7-1 Fujishiro-dai, Suita, Osaka 565-8565, Japan. E-mail: wshimizu@hsp.ncvc.go.jp.

REFERENCES

1. Brugada P, Brugada J. Right bundle branch block, persistent ST segment elevation and sudden cardiac death: a distinct clinical and electrocardiographic syndrome: a multicenter report. J Am Coll Cardiol 1992;20:1391–6.
2. Smits JP, Eckardt L, Probst V, et al. Genotype-phenotype relationship in Brugada syndrome: electrocardiographic features differentiate *SCN5A*-related patients from non- *SCN5A*-related patients. J Am Coll Cardiol 2002;40:350–6.
3. Tukkie R, Sogaard P, Vleugels J, de Groot IK, Wilde AA, Tan HL. Delay in right ventricular activation contributes to Brugada syndrome. Circulation 2004;109:1272–7.
4. Shimizu W, Aiba T, Kamakura S. Mechanisms of disease: current understanding and future challenges in Brugada syndrome. Nat Clin Pract Cardiovasc Med 2005;2:408–14.
5. Yan GX, Antzelevitch C. Cellular basis for the Brugada syndrome and other mechanisms of arrhythmogenesis associated with ST-segment elevation. Circulation 1999;100:1660–6.
6. Antzelevitch C, Brugada P, Borggrefe M, et al. Brugada syndrome. Report of the second consensus conference: endorsed by the Heart Rhythm Society and the European Heart Rhythm Association. Circulation 2005;111:659–70.
7. Probst V, Veltmann C, Eckardt L, et al. Long-term prognosis of patients diagnosed with Brugada syndrome: results from the FINGER Brugada syndrome registry. Circulation 2010;121:635–43.
8. Miyazaki T, Mitamura H, Miyoshi S, Soejima K, Aizawa Y, Ogawa S. Autonomic and antiarrhythmic drug modulation of ST segment elevation in patients with Brugada syndrome. J Am Coll Cardiol 1996;27:1061–70.
9. Lahiri MK, Kannankeril PJ, Goldberger JJ. Assessment of autonomic function in cardiovascular disease. J Am Coll Cardiol 2008;51:1725–33.
10. Arai Y, Saul JP, Albrecht P, et al. Modulation of cardiac autonomic activity during and immediately after exercise. Am J Physiol 1989;256: H132–41.
11. Litovsky SH, Antzelevitch C. Differences in the electrophysiological response of canine ventricular subendocardium and subepicardium to acetylcholine and isoproterenol. A direct effect of acetylcholine in ventricular myocardium. Circ Res 1990;67:615–27.
12. Papadakis M, Petzer E, Sharma S. Unmasking of the Brugada phenotype during exercise testing and its association with ventricular arrhythmia on the recovery phase. Heart 2009;95:2022.
13. Amin AS, de Groot EA, Ruijter JM, Wilde AA, Tan HL. Exercise-induced ECG changes in Brugada syndrome. Circ Arrhythm Electrophysiol 2009;2:531–9.
14. Noda T, Shimizu W, Taguchi A, et al. ST-segment elevation and ventricular fibrillation without coronary spasm by intracoronary injection of acetylcholine and/or ergonovine maleate in patients with Brugada syndrome. J Am Coll Cardiol 2002;40:1841–7.
15. Ikeda T, Abe A, Yusu S, et al. The full stomach test as a novel diagnostic technique for identifying patients at risk of Brugada syndrome. J Cardiovasc Electrophysiol 2006;17:602–7.
16. Yokokawa M, Okamura H, Noda T, et al. Neurally-mediated syncope as a cause of syncope in patients with Brugada electrocardiogram. J Cardiovasc Electrophysiol 2010;21:186–92.
17. Savin WM, Davidson DM, Haskell WL. Autonomic contribution to heart rate recovery from exercise in humans. J Appl Physiol 1982;53: 1572–5.
18. Imai K, Sato H, Hori M, et al. Vagally mediated heart rate recovery after exercise is accelerated in athletes but blunted in patients with chronic heart failure. J Am Coll Cardiol 1994;24:1529–35.
19. Scornik FS, Desai M, Brugada R, et al. Functional expression of "cardiac-type" Nav1.5 sodium channel in canine intracardiac ganglia. Heart Rhythm 2006;3:842–50.
20. Veldkamp MW, Viswanathan PC, Bezzina C, Baartscheer A, Wilde AA, Balser JR. Two distinct congenital arrhythmias evoked by a multidysfunctional Na+ channel. Circ Res 2000;86:e91–7.
21. Clancy CE, Rudy Y. Na^+ channel mutation that causes both Brugada and long-QT syndrome phenotypes. A stimulation study of mechanism. Circulation 2002;105:1208–13.
22. Dumaine R, Towbin JA, Brugada P, et al. Ionic mechanisms responsible for the electrocardiographic phenotype of the Brugada syndrome are temperature dependent. Circ Res 1999;85:803–9.
23. Epstein AE, Dimarco JP, Ellenbogen KA, et al. ACC/AHA/HRS 2008 guidelines for device-based therapy of cardiac rhythm abnormalities: a report of the American College of Cardiology/American Heart Association Task Force on Practice Guidelines (Writing Committee to Revise the ACC/AHA/NASPE 2002 Guideline Update for Implantation of Cardiac Pacemakers and Antiarrhythmia Devices). J Am Coll Cardiol 2008;51:e1–62.
24. Kamakura S, Ohe T, Nakazawa K, et al., for the Brugada Syndrome Investigators in Japan. Long-term prognosis of probands with Brugada-pattern ST-elevation in leads V1-V3. Circ Arrhythm Electrophysiol 2009;2:495–503.
25. Brugada J, Brugada R, Antzelevitch C, Towbin J, Nademanee K, Brugada P. Long term follow-up of individuals with the electrocardiographic pattern of right bundle-branch block and ST-segment elevation in precordial leads V1 to V3. Circulation 2002;105:73–8.
26. Brugada P, Brugada R, Mont L, Rivero M, Geelen P, Brugada J. Natural history of Brugada syndrome: the prognostic value of programmed electrical stimulation of the heart. J Cardiovasc Electrophysiol 2003;14:455–7.
27. Priori SG, Napolitano C, Gasparini M, et al. Natural history of Brugada syndrome: insights for risk stratification and management. Circulation 2002;105:1342–7.
28. Ikeda T, Takami M, Sugi K, Mizusawa Y, Sakurada H, Yoshino H. Noninvasive risk stratification of subjects with a Brugada-type electrocardiogram and no history of cardiac arrest. Ann Noninvasive Electrocardiol 2005;10:396–403.
29. Paul M, Gerss J, Schulze-Bahr E, et al. Role of programmed ventricular stimulation in patients with Brugada syndrome: a meta-analysis of worldwide published data. Eur Heart J 2007;17:2126–33.
30. Eckardt L, Probst V, Smits JP, et al. Long-term prognosis of individuals with right precordial ST-segment-elevation Brugada syndrome. Circulation 2005;111:257–63.
31. Sacher F, Probst V, Iesaka Y, et al. Outcome after implantation of a cardioverter-defibrillator in patients with Brugada syndrome: a multicenter study. Circulation 2006;114:2317–24.

Key Words: Brugada syndrome ■ exercise testing ■ ST-segment elevation.

KCNE2 modulation of Kv4.3 current and its potential role in fatal rhythm disorders

Jie Wu, PhD,* Wataru Shimizu, MD, PhD,† Wei-Guang Ding, MD, PhD,‡ Seiko Ohno, MD, PhD,§ Futoshi Toyoda, PhD,‡ Hideki Itoh, MD, PhD,¶ Wei-Jin Zang, MD, PhD,* Yoshihiro Miyamoto, MD, PhD,‖ Shiro Kamakura, MD, PhD,† Hiroshi Matsuura, MD, PhD,‡ Koonlawee Nademanee, MD, FACC,# Josep Brugada, MD,** Pedro Brugada, MD,†† Ramon Brugada, MD, PhD, FACC,‡‡ Matteo Vatta, PhD,§§¶¶ Jeffrey A. Towbin, MD, FAAP, FACC,§§ Charles Antzelevitch, PhD, FACC, FAHA, FHRS,‖‖ Minoru Horie, MD, PhD¶

*From the *Pharmacology Department, Medical School of Xi'an Jiaotong University. Xi'an, Shaanxi, China, †Division of Cardiology, Department of Internal Medicine, National Cardiovascular Center, Suita, Japan, ‡Department of Physiology, Shiga University of Medical Science, Ohtsu, Japan, §Department of Cardiovascular Medicine, Kyoto University of Graduate School of Medicine, Kyoto, Japan, ¶Department of Cardiovascular Medicine, Shiga University of Medical Science, Shiga, Japan, ‖Laboratory of Molecular Genetics, National Cardiovascular Center, Suita, Japan, #Department of Medicine (Cardiology), University of Southern California, Los Angeles, California, **Cardiovascular Institute, Hospital Clinic, University of Barcelona, Barcelona, Spain, ††Heart Rhythm Management Centre, Free University of Brussels (UZ Brussel) VUB, Brussels, Belgium, ‡‡School of Medicine, Cardiovascular Genetics Center, University of Girona, Girona, Spain, §§Departments of Pediatrics, Baylor College of Medicine, Houston, Texas, ¶¶Department of Molecular Physiology and Biophysics, Baylor College of Medicine, Houston, Texas, and ‖‖Masonic Medical Research Laboratory, Utica, New York.*

BACKGROUND The transient outward current I_{to} is of critical importance in regulating myocardial electrical properties during the very early phase of the action potential. The auxiliary β subunit *KCNE2* recently was shown to modulate I_{to}.

OBJECTIVE The purpose of this study was to examine the contributions of *KCNE2* and its two published variants (M54T, I57T) to I_{to}.

METHODS The functional interaction between Kv4.3 (α subunit of human I_{to}) and wild-type (WT), M54T, and I57T *KCNE2*, expressed in a heterologous cell line, was studied using patch-clamp techniques.

RESULTS Compared to expression of Kv4.3 alone, co-expression of WT *KCNE2* significantly reduced peak current density, slowed the rate of inactivation, and caused a positive shift of voltage dependence of steady-state inactivation curve. These modifications rendered Kv4.3 channels more similar to native cardiac I_{to}. Both M54T and I57T variants significantly increased I_{to} current density and slowed the inactivation rate compared with WT *KCNE2*. Moreover, both variants accelerated the recovery from inactivation.

CONCLUSION The study results suggest that *KCNE2* plays a critical role in the normal function of the native I_{to} channel complex in human heart and that M54T and I57T variants lead to a gain of function of I_{to}, which may contribute to generating potential arrhythmogeneity and pathogenesis for inherited fatal rhythm disorders.

KEYWORDS Cardiac arrhythmia; M54T variation; I57T variation; *KCNE2*; Kv4.3; Sudden cardiac death

ABBREVIATIONS CHO = Chinese hamster ovary; **HERG** = human ether-a-go-go related gene; **WT** = wild type

(Heart Rhythm 2010;7:199–205)

Introduction

Classic voltage-gated K^+ channels consist of four pore-forming (α) subunits that contain the voltage sensor and ion selectivity filter[1,2] and accessory regulating (β) subunits.[3] *KCNE* family genes encode several kinds of β subunits consisting of single transmembrane-domain peptides that co-assemble with α subunits to modulate ion selectivity, gating kinetics, second messenger regulation, and the pharmacology of K^+ channels. Association of the *KCNE1* product minK with the α subunit Kv7.1 encoding *KCNQ1* forms the slowly activating delayed rectifier K^+ current I_{Ks} in the heart.[4,5] In contrast, association of the *KCNE2* product MiRP1 with the human ether-a-go-go related gene (HERG) forms the cardiac rapid delayed rectifier K^+ current I_{Kr}.[6]

The first two authors contributed equally to the original concept and the authorship of this study. This study was supported by grants from the Ministry of Education, Culture, Sports, Science, Technology Leading Project for Biosimulation to Dr. Horie; Health Sciences Research grants (H18-Research on Human Genome-002) from the Ministry of Health, Labour and Welfare, Japan to Drs. Shimizu and Horie; the National Natural Science Foundation of China (Key Program, No.30930105; General Program, No. 30873058, 30770785) and the National Basic Research Program of China (973 Program, No. 2007CB512005) and CMB Distinguished Professorships Award (No. F510000/G16916404) to Dr. Zang; and National Institutes of Health Grant HL47678 and Free and Accepted Masons of New York State and Florida to Dr. Antzelevitch. **Address reprint requests and correspondence:** Dr. Minoru Horie, Department of Cardiovascular and Respiratory Medicine, Shiga University of Medical Science, Otsu, Shiga 520-2192, Japan. E-mail address: horie@belle.shiga-med.ac.jp. (Received August 20, 2009; accepted October 7, 2009.)

1547-5271/$ -see front matter doi:10.1016/j.hrthm.2009.10.012

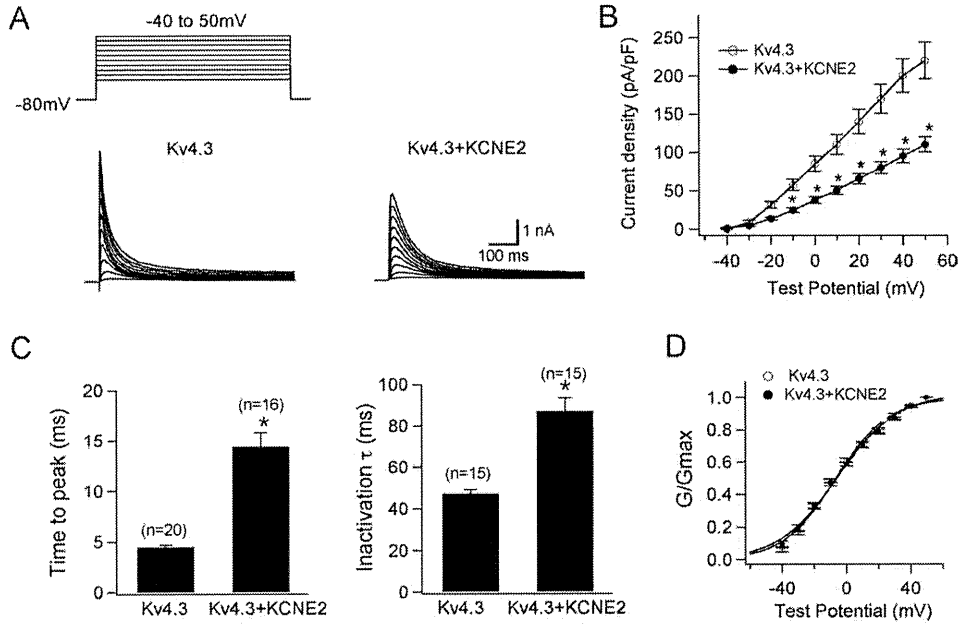

Figure 1 *KCNE2* co-expression with Kv4.3 produces smaller I_{to}-like currents with slower activation/inactivation kinetics. **A:** Representative current traces recorded from Chinese hamster ovary (CHO) cells expressing Kv4.3 **(left)** and Kv4.3 + *KCNE2* **(right).** As shown in the **inset** in panel A, depolarizing step pulses of 1-second duration were introduced from a holding potential of −80 mV to potentials ranging from −40 to +50 mV in 10-mV increments. **B:** Current–voltage relationship curve showing peak current densities in the absence and presence of co-transfected *KCNE2* (*P <.05 vs Kv4.3). **C:** Bar graphs showing the kinetic properties of reconstituted channel currents: time to peak of activation course **(left)** and inactivation time constants **(right)** measured using test potential to +20 mV (*P <.05 vs Kv4.3). Numbers in parentheses indicate numbers of experiments. **D:** Normalized conductance–voltage relationship for peak outward current of Kv4.3 and Kv4.3 + *KCNE2* channels.

Abbott et al reported that three *KCNE2* variants (Q9E, M54T, I57T) caused a loss of function in I_{Kr} and thereby were associated with the congenital or drug-induced long QT syndrome.[6,7] However, the reported QTc values in two index patients with M54T and I57T variants, both located in the transmembrane segment of MiRP1, were only mildly prolonged (390–500 ms and 470 ms).[6] We recently identified the same missense *KCNE2* variant, I57T, in which isoleucine was replaced by threonine at codon 57, in three unrelated probands showing a Brugada type 1 ECG. These findings are difficult to explain on the basis of a loss of function in I_{Kr}, thus leading us to explore other mechanisms.

Recent studies have demonstrated that interaction between α and β subunits (*KCNE*s) of voltage-gated K^+ channel is more promiscuous; for example, MiRP1 has been shown to interact with Kv7.1,[8–10] HCN1,[11] Kv2.1,[12] and Kv4.2.[13] These studies suggest that MiRP1 may also co-associate with Kv4.3 and contribute to the function of transient outward current (I_{to}) channels.[14] Indeed, a recent study reported that I_{to} is diminished in *kcne2* (–/–) mice.[15]

In the human heart, I_{to} currents are of critical importance in regulating myocardial electrical properties during the very early phase of the action potential and are thought to be central to the pathogenesis of Brugada-type ECG manifestations.[16] Antzelevitch et al demonstrated that a gain of function in I_{to} secondary to a mutation in *KCNE3* contributes to a Brugada phenotype by interacting with Kv4.3 and thereby promoting arrhythmogenicity.[14]

We hypothesized that mutations in *KCNE2* may have similar actions and characterize the functional consequences of interaction of wild-type (WT) and two mutant (I57T, M54T) MiRP1 with Kv4.3[17,18] using heterologous co-expression of these α and β subunits in Chinese hamster ovary (CHO) cells.

Methods

Heterologous expression of hKv4.3 and β subunits in CHO cells

Full-length cDNA fragment of *KCNE2* in pCR3.1 vector[10] was subcloned into pIRES-CD8 vector. This expression vector is useful in cell selection for later electrophysiologic study (see below). Two *KCNE2* mutants (M54T, I57T) were constructed using a Quick Change II XL site-directed mutagenesis kit according to the manufacturer's instructions (Stratagene, La Jolla, CA, USA) and subcloned to the same vector. Two *KCNE2* mutants were fully sequenced (ABI3100x, Applied Biosystems, Foster City, CA, USA) to ensure fidelity. Full-length cDNA encoding the short isoform of human Kv4.3 subcloned into the pIRES-GFP (Clontech, Palo Alto, CA, USA) expression vector was kindly provided by Dr. G.F. Tomaselli (Johns Hopkins University). Full-length cDNA encoding Kv channel-interacting protein (*KCNIP2*) subcloned into the PCMV-IRS expression vector was a kind gift from Dr. G.-N. Tseng (Virginia Commonwealth University). *KCND3* was transiently transfected into CHO cells together with *KCNE2* (or M54T or I57T) cDNA at equimolar ratio (*KCND3* 1.5 μg,

Table 1 Effects of *KCNE2* on Kv4.3 and Kv4.3 + KChIP2b

Parameter	Kv4.3	Kv4.3 *KCNE2*	Kv4.3 KChIP2b	Kv4.3 KChIP2b *KCNE2*
Current density at +20 mV (pA/pF)	142.0 ± 16.0 (n = 12)	66.0 ± 6.6* (n = 12)	191.5 ± 33.8 (n = 15)	77.8 ± 5.9† (n = 20)
Steady-state activation ($V_{0.5}$ in mV)	−6.5 ± 2.1 (n = 9)	−5.5 ± 1.7 (n = 11)	−7.5 ± 1.7 (n = 8)	−7.4 ± 1.4 (n = 8)
Steady-state inactivation ($V_{0.5}$ in mV)	−46.0 ± 1.3 (n = 10)	−40.8 ± 1.7* (n = 8)	−49.8 ± 1.4 (n = 7)	−44.5 ± 1.9† (n = 7)
τ of inactivation at +20 mV (τ_{inact} in ms)	47.3 ± 2.0 (n = 15)	87.2 ± 6.2* (n = 15)	47.5 ± 2.2 (n = 15)	66.6 ± 3.5† (n = 15)
Time to peak at +50 mV (TtP in ms)	4.5 ± 0.2 (n = 20)	14.4 ± 1.4* (n = 16)	4.1 ± 0.2 (n = 15)	6.1 ± 0.5† (n = 21)
τ of recovery from inactivation (ms)	419.6 ± 18.8 (n = 6)	485.6 ± 74.8 (n = 6)	89.2 ± 5.3 (n = 6)	60.2 ± 6.9† (n = 6)

*Significantly different from Kv4.3.
†Significantly different from Kv4.3 + KChIP2b.

KCNE2 1.5 μg) using Lipofectamine (Invitrogen Life Technologies, Carlsbad, CA, USA) according to the manufacturer's instructions. In one set of experiments, we also co-transfected equimolar levels of KChIP2b (*KCND3* 1.5 μg, *KCNE2* 1.5 μg, *KCNIP2* 1.5 μg). The transfected cells were then cultured in Ham's F-12 medium (Nakalai Tesque, Inc., Kyoto, Japan) supplemented with 10% fetal bovine serum (JRH Biosciences, Inc., Lenexa, KS, USA) and antibiotics (100 international units per milliliter penicillin and 100 μg/mL streptomycin) in a humidified incubator gassed with 5% CO_2 and 95% air at 37°C. The cultures were passaged every 4 to 5 days using a brief trypsin-EDTA treatment. The trypsin-EDTA treated cells were seeded onto glass coverslips in a Petri dish for later patch-clamp experiments.

Electrophysiologic recordings and data analysis

After 48 hours of transfection, a coverslip with cells was transferred to a 0.5-mL bath chamber at 25°C on an inverted microscope stage and perfused at 1 to 2 mL/min with extracellular solution containing the following (in mM): 140 NaCl, 5.4 KCl, 1.8 $CaCl_2$, 0.5 $MgCl_2$, 0.33 NaH_2PO_4, 5.5 glucose, and 5.0 HEPES; pH 7.4 with NaOH. Cells that emitted green fluorescence were chosen for patch-clamp experiments. If co-expressed with *KCNE2* (or its mutants), the cells were incubated with polystyrene microbeads precoated with anti-CD8 antibody (Dynabeads M450, Dynal, Norway) for 15 minutes. In these cases, cells that emitted green fluorescence and had attached beads were chosen for electrophysiologic recording. Whole-cell membrane currents were recorded with an EPC-8 patch-clamp amplifier (HEKA, Lambrecht, Germany), and data were low-pass filtered at 1 kHz, acquired at 5 kHz through an LIH-1600 analog-to-digital converter (HEKA), and stored on hard disk using PulseFit software (HEKA). Patch pipettes were fabricated from borosilicate glass capillaries (Narishige, Tokyo, Japan) using a horizontal microelectrode puller (P-97, Sutter Instruments, Novato, CA, USA) and the pipette tips fire-polished using a microforge. Patch pipettes had a resistance of 2.5 to 5.0 MΩ when filled with the following pipette solution (in mM): 70 potassium aspartate, 50 KCl, 10 KH_2PO_4, 1 $MgSO_4$, 3 Na_2-ATP (Sigma, Japan, Tokyo), 0.1 Li_2-GTP (Roche Diagnostics GmbH, Mannheim, Germany), 5 EGTA, and 5 HEPES (pH 7.2).

Cell membrane capacitance (C_m) was calculated from 5 mV-hyperpolarizing and depolarizing steps (20 ms) applied from a holding potential of −80 mV according to Equation 1[19]:

$$C_m = \tau_c I_0/\Delta V_m(1 - I_\infty/I_0), \quad (1)$$

where τ_c = time constant of capacitance current relaxation, I_0 = initial peak current amplitude, ΔV_m = amplitude of voltage step, and I_∞ = steady-state current value. Whole-cell currents were elicited by a family of depolarizing voltage steps from a holding potential of −80 mV. The difference between the peak current amplitude and the current at the end of a test pulse (1-second duration) was referred to as the transient outward current. To control for cell size variability, currents were expressed as densities (pA/pF).

Steady-state activation curves were obtained by plotting the normalized conductance as a function of peak outward potentials. Steady-state inactivation curves were generated by a standard two-pulse protocol with a conditioning pulse of 500-ms duration and obtained by plotting the normalized current as a function of the test potential. Steady-state inactivation/activation kinetics were fitted to the following Boltzmann equation (Eq. 2):

$$Y(V) = 1/(1 + \exp[(V_{1/2} - V)/k]), \quad (2)$$

where Y = normalized conductance or current, $V_{1/2}$ = potential for half-maximal inactivation or activation, respectively, and k = slope factor.

Data relative to inactivation time constants, time to peak, and mean current levels were obtained by using current data recorded at +50 mV or +20 mV. Recovery from inactivation was assessed by a standard paired-pulse protocol: a 400-ms test pulse to +50 mV (P1) followed by a variable

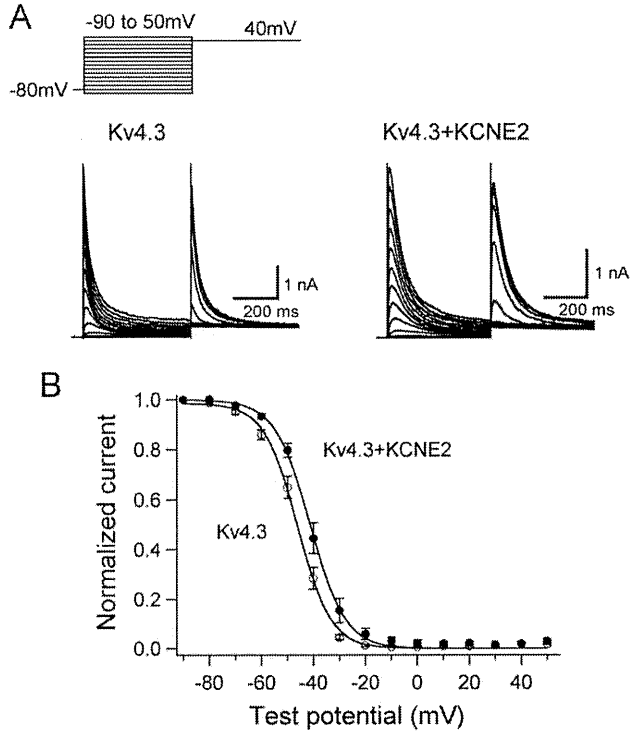

Figure 2 *KCNE2* co-expression with Kv4.3 causes a positive shift of voltage dependence of steady-state inactivation. **A:** Representative Kv4.3 and Kv4.3 + *KCNE2* current traces induced by 500-ms pulses (P1) from −90 to +50 mV applied from the holding potential −80 mV in 10-mV steps followed by a second pulse (P2) to +40 mV. **B:** Steady-state inactivation curves for Kv4.3 *(open circles)* and Kv4.3 + *KCNE2 (closed circles)* channels.

recovery interval at −80 mV and then a second test pulse to +50 mV (P2). Both the inactivation time constants and the time constant for recovery from inactivation were determined by fitting the data to a single exponential (Eq. 3):

$$I(t) \text{ (or P2/P1)} = A + B_{exp}(-t/\tau), \quad (3)$$

where I(t) = current amplitude at time t, A and B = constants, and τ = inactivation time constant or time constant for recovery from inactivation. For measurement of recovery from inactivation, the plot of P2/P1 instead of I(t) was used.

All data were given as mean ± SEM. Statistical comparisons between two groups were analyzed using Student's unpaired t-test. Comparisons among multiple groups were analyzed using analysis of variance followed by Dunnett test. $P < .05$ was considered significant.

Results

Effects of *KCNE2* on Kv4.3 currents and its gating kinetics

WT *KCNE2* initially was co-expressed with *KCND3*, the gene encoding Kv4.3, the α subunit of the I_{to} channel,[17,18] in CHO cells. Figure 1A shows representative whole-cell current traces recorded from cells transfected with *KCND3* and co-transfected with (right) or without (left) *KCNE2*. Cells expressing Kv4.3 channels alone showed rapidly activating and inactivating currents. Co-expression of *KCNE2* significantly reduced peak current densities as summarized in the current–voltage relationship curve shown in Figure 1B and slowed both activation and inactivation kinetics (Table 1). Figure 1C (left) shows mean time intervals from the onset of the pulse to maximum current (time to peak), whereas the right panel shows time constants of inactivation (at +20 mV) obtained using Equation 3. Thus, co-transfection of *KCNE2* significantly increased both the time to peak and the time constant.

In contrast, *KCNE2* did not affect the voltage dependence of steady-state activation as assessed by plotting the normalized conductance as a function of test potential (Figure 1D). Fitting to the Boltzmann equation (Eq. 2) yielded half-maximal activation potentials of −6.5 ± 2.1 mV for Kv4.3 alone (open circles) and −5.5 ± 1.7 mV for Kv4.3 + *KCNE2* channels (filled circles, P = NS; Table 1). These findings are consistent with those previously reported for studies using *Xenopus* oocytes, CHO cells, and HEK293 cells.[20,21]

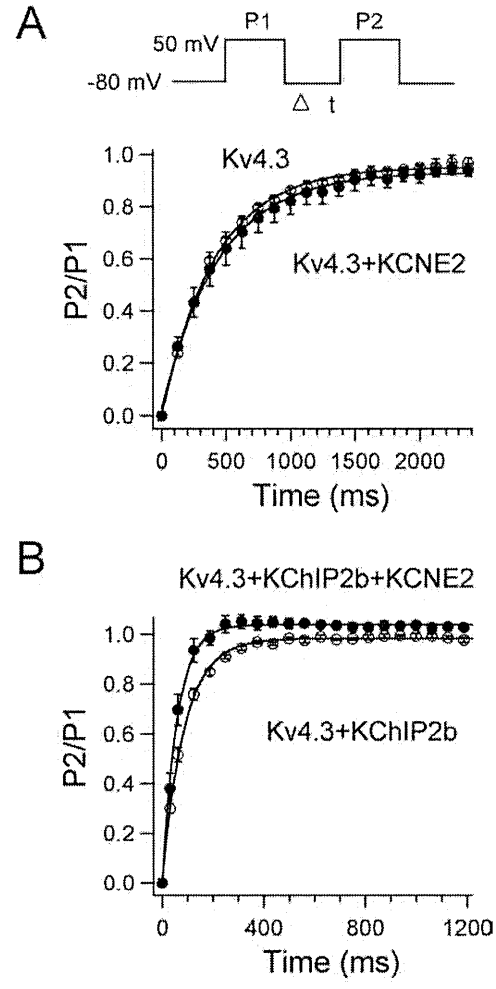

Figure 3 Effects of *KCNE2* co-expression on recovery from inactivation of Kv4.3 **(A)** and Kv4.3 + KChIP2b **(B)** currents. Recovery from inactivation was assessed by a two-pulse protocol **(A, inset):** a 400-ms test pulse to +50 mV (P1) followed by a variable interval at −80 mV, then by a second test pulse to +50 mV (P2). Data were fit to a single exponential.

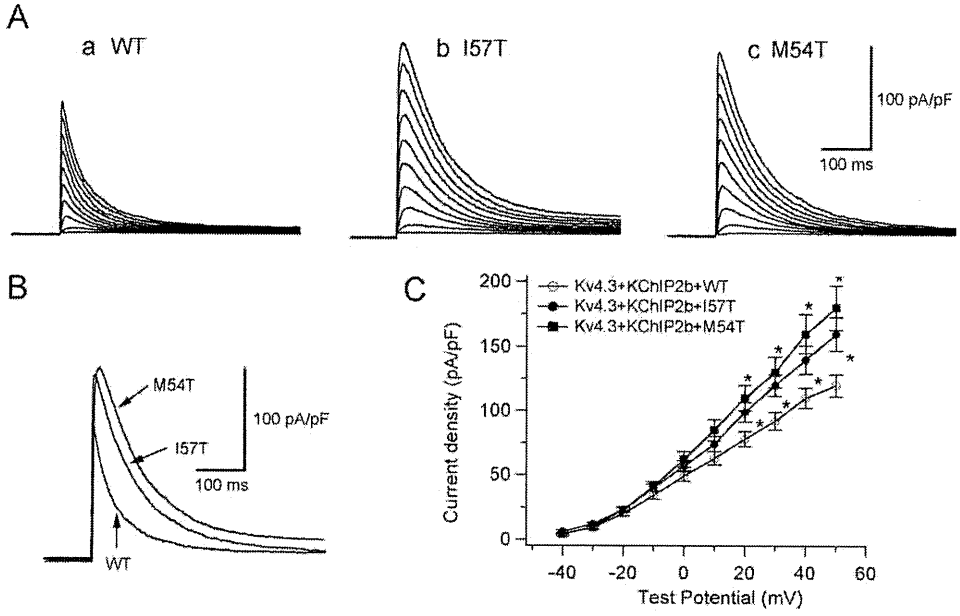

Figure 4 Two *KCNE2* transmembrane variants, I57T and M54T, increase the reconstituted Kv4.3 + KChIP2b channel current and slow its inactivation. **A:** Three sets of current traces elicited by depolarizing pulses for 500 ms from a holding potential of −80 mV to potentials ranging between −40 and +50 mV in 10-mV increments (same protocol as in experiments of Figure 1A). **B:** Superimposition of three original current traces recorded upon depolarization showing variant-related increase in peak outward current density. **C:** Current–voltage relationship curve showing average peak outward current densities (*P <.05 vs Kv4.3 + KChIP2b + WT). WT = wild type.

KCNE2 co-expression also caused a positive shift (approximately +5 mV) of voltage dependence of steady-state inactivation. Steady-state inactivation was assessed using a double-step pulse method (Figure 2A, inset). Peak outward currents recorded at various levels of prepulse (Figure 2A) were normalized by that measured after a 500-ms prepulse at −90 mV and are plotted as a function of prepulse test potentials (Figure 2B). Half-inactivation potentials of steady-state inactivation, determined by fitting data to the Boltzmann equation (Eq. 2), were −46.0 ± 1.3 mV for Kv4.3 (open circles) and −40.8 ± 1.7 mV for Kv4.3 + *KCNE2* (filled circles, P <.01), consistent with the observation of Tseng's group.[13]

A double-pulse protocol (Figure 3A, inset) was used to test the effect of *KCNE2* co-expression on the time course for recovery from inactivation. Figure 3A shows the time course of recovery of Kv4.3 alone (open circles) and Kv4.3 + *KCNE2* (filled circles). Mean time constants for recovery from inactivation were not significantly different, indicating that co-transfection of *KCNE2* did not affect the time course of recovery from inactivation.

Effects of *KCNE2* on Kv4.3 + KChIP2b current and its gating kinetics

For human native cardiac I_{to}, KChIP2 has been shown to serve as a principal β subunit.[22–25] Accordingly, in another series of experiments, we examined the effect of WT and mutant *KCNE2* on Kv4.3 + KChIP2b current. Consistent with previous reports, in the presence of KChIP2, Kv4.3 currents showed a significantly faster recovery from inactivation (Figure 3B and Table 1).[26,27] Co-expression of WT *KCNE2* produced similar changes on Kv4.3 + KChIP2b current as on Kv4.3 current (Table 1). Kv4.3 + KChIP2b current recovery from inactivation was further accelerated: average time constant was 89.2 ± 6.5 ms for Kv4.3 + KChIP2b alone (open circles) and 60.2 ± 8.4 ms for Kv4.3 + KChIP2b + *KCNE2* (filled circles, P <.05). In 16 of 21 cells transfected with *KCNE2*, we observed an "overshoot" phenomenon, which is commonly seen during recording of native I_{to} in human ventricular myocytes.[28]

KCNE2 variants increase Kv4.3 + KChIP2b current and alter its gating kinetics

The I57T variant was first identified in an asymptomatic middle-aged woman with very mild QT prolongation.[6] In addition to this variant, the authors reported another *KCNE2* variant of the transmembrane segment (M54T) that was associated with ventricular fibrillation during exercise in a middle-aged woman. This patient appeared to show a wide range of QTc interval (390–500 ms). Therefore, we tested the functional effects of these two transmembrane *KCNE2* variants on Kv4.3 + KChIP2b currents.

The three panels of Figure 4A show three sets of current traces elicited by depolarizing pulses from a holding potential of −80 mV in cells co-transfected with WT (a), I57T (b), or M54T (c) *KCNE2*. Neither variant caused a significant shift of half-maximal activation voltage: −7.4 ± 1.4 mV (n = 8) for co-expression of WT *KCNE2*, −6.1 ± 1.5 mV (n = 8) for I57T, and −6.6 ± 1.6 mV (n = 8) for M54T. Both variants significantly increased I_{to} density: 125.0 ± 10.6 pA/pF in WT *KCNE2* (n = 21), 178.1 ± 12.1 pA/pF with I57T (n = 9), and 184.3 ± 27.9 pA/pF with M54T (n = 9, Figure 4C).

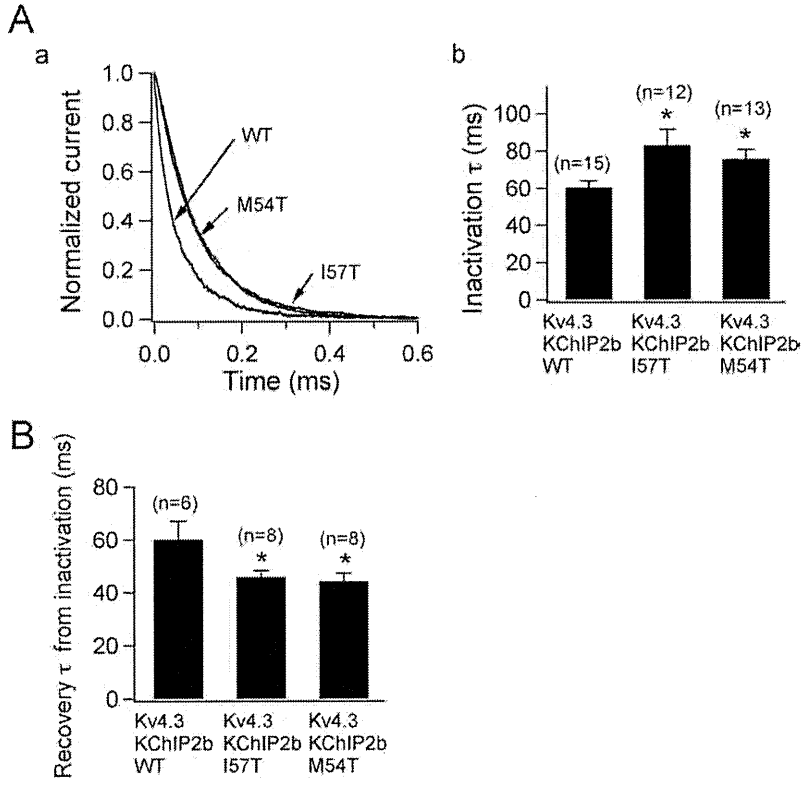

Figure 5 Two *KCNE2* variants slow inactivation kinetics and accelerate recovery from inactivation. **A, a:** Three current traces obtained from Chinese hamster ovary (CHO) cells transfected with wild-type (WT), I57T, and M54T *KCNE2* variant co-expressed with Kv4.3 and KChIP2b. Traces, which are normalized and superimposed, show that the variants slow inactivation. **A, b:** Time constants of decay at +20 mV for WT and variant *KCNE2* (*P <.05 vs Kv4.3 + KChIP2b + WT). Numbers in parentheses indicate numbers of observations. **B:** Time constants of recovery from inactivation recorded using a double-pulse protocol (*P <.05 vs Kv4.3 + KChIP2b + WT). Numbers in parentheses indicate numbers of observations.

Figure 5A shows the three traces depicted in Figure 4B normalized to their peak current level. This representation shows that the time course of inactivation of the two variant currents is slowed. The current decay was fitted by Equation 3 and the time constants (at +20 mV) summarized in Figure 5A, panel b. Finally, Figure 5B shows that the time constants of recovery of the two mutant channels from inactivation were significantly reduced. Thus, compared to WT *KCNE2*, recovery of reconstituted Kv4.3 + KChIP2b channels from inactivation was significantly accelerated with both I57T and M54T mutants.

Discussion

Kv4.3/KChIP2/MiRP1 complex can recapitulate the native I_{to}

In the present study, co-expression of WT *KCNE2* produced changes in kinetic properties (Figures 1–3 and Table 1) that led to close recapitulation of native cardiac I_{to}.[28,29] Notably, in addition to causing a positive shift of steady-state inactivation (Figure 2), *KCNE2* co-expression hastened the recovery of Kv4.3 + KChIP2b channels from inactivation (Figure 3). These modifications rendered Kv4.3 + KChIP2b channels more similar to native cardiac I_{to}, suggesting that *KCNE2* may be an important component of the native I_{to} channel complex. In contrast to a previous observation in HEK293 cells,[21] *KCNE2* co-expression decreased the current density of Kv4.3 and Kv4.3 + KChIP2b channel current in the present study, which seems to be a more reasonable result as the native I_{to} density reportedly was smaller in isolated human heart.[28] *KCNE2* co-expression has also been shown to reduce the density of Kv7.1[8,9] and HERG[6,7] channels.

Similar to the result of Deschenes and Tomaselli,[21] we failed to observe an overshoot during recovery from inactivation when *KCNE2* was co-expressed with Kv4.3 (Figure 3A), which is in contrast to the report of another group.[13] However, co-expression of *KCNE2* with Kv4.3 + KChIP2 channels produced an overshoot (Figure 3B), consistent with the report of Wettwer's group.[25] Wettwer et al also found that other *KCNE* subunits either were ineffective or induced only a small overshoot in CHO cells. Therefore, both MiRP1 and KChIP2 subunits are sufficient and necessary to recapitulate native I_{to} in the heart. Considering that the overshoot phenomenon has been described only in human ventricular I_{to} channels of the epicardial but not endocardial region,[28] these results may further implicate participation of MiRP1 and KChIP2 in the I_{to} channel complex in epicardium.

KCNE2 variants may alter the arrhythmogenic substrate by modulating I_{to}

Heterologous expression in CHO cells was conducted to examine the functional effects of I57T and M54T variants on Kv4.3 + KChIP2 channels. Both I57T and M54T

KCNE2 variants significantly (1) increased peak transient outward current density (Figure 4), (2) slowed the decay of the reconstituted I_{to} (Figure 5A), and (3) accelerated its recovery from inactivation (Figure 5B). Both variants thus caused an important gain of function in human I_{to}. These sequence changes may play a role in modulating I_{to} and thereby predispose to some inherited fatal rhythm disorders.

Functional effects on I_{to} induced by I57T and M54T resemble each other, increasing I_{to} density and accelerating its recovery from inactivation. The gain of function in I_{to} opposes the fast inward Na^+ currents during phase 0 of the action potential, leading to all or none repolarization at the end of phase 1 and loss of the epicardial action potential dome, thus promoting phase 2 reentry and fatal ventricular arrhythmias.[30]

Another *KCNE2* variant (M54T) associated with fatal arrhythmias was first identified in a woman who had a history of ventricular fibrillation and varied QT intervals.[6] It is possible that her arrhythmia was also related to a gain of function in I_{to} secondary to this variation in *KCNE2*. Interestingly, the I57T variant has been reported to produce a loss of function of HERG or Kv7.1 channels, thereby predisposing to long QT syndrome,[6,8] indicating that the same *KCNE2* variant could cause two different cardiac rhythm disorders, similar to long QT syndrome and Brugada syndrome caused by *SCN5A* mutations.[31,32]

References

1. Kass RS, Freeman LC. Potassium channels in the heart: cellular, molecular, and clinical implications. Trends Cardiovasc Med 1993;3:149–159.
2. MacKinnon R. Determination of the subunit stoichiometry of a voltage-activated potassium channel. Nature 1991;350:232–235.
3. Abbott GW, Goldstein SA. A superfamily of small potassium channel subunits: form and function of the MinK-related peptides (MiRPs). Q Rev Biophys 1998;31:357–398.
4. Barhanin J, Lesage F, Guillemare E, Fink M, Lazdunski M, Romey G. KvLQT1 and IsK (minK) proteins associate to form the I_{Ks} cardiac potassium current. Nature 1996;384:78–80.
5. Sanguinetti MC, Curran ME, Zou AR, et al. Coassembly of KvLQT1 and minK (I_{Ks}) proteins to form cardiac I_{Ks} potassium channel. Nature 1996; 384:80–83.
6. Abbott GW, Sesti F, Splawski I, et al. MiRP1 forms I_{Kr} potassium channels with HERG and is associated with cardiac arrhythmia. Cell 1999;97:175–187.
7. Sesti F, Abbott GW, Wei J, et al. A common polymorphism associated with antibiotic-induced cardiac arrhythmia. Proc Natl Acad Sci U S A 2000;97: 10613–10618.
8. Tinel N, Diochot S, Borsotto M, Lazdunski M, Barhanin J. *KCNE2* confers background current characteristics to the cardiac KCNQ1 potassium channel. EMBO J 2000;19:6326–6330.
9. Wu DM, Jiang M, Zhang M, Liu XS, Korolkova YV, Tseng GN. *KCNE2* is colocalized with KCNQ1 and *KCNE1* in cardiac myocytes and may function as a negative modulator of $I_{(Ks)}$ current amplitude in the heart. Heart Rhythm 2006;3:1469–1480.
10. Toyoda F, Ueyama H, Ding WG, Matsuura H. Modulation of functional properties of KCNQ1 channel by association of KCNE1 and KCNE2. Biochem Biophys Res Commun 2006;344:814–820.
11. Yu H, Wu J, Potapova I, et al. MinK-related peptide 1: a beta subunit for the HCN ion channel subunit family enhances expression and speeds activation. Circ Res 2001;88:E84–E87.
12. McCrossan ZA, Roepke TK, Lewis A, Panaghie G, Abbott GW. Regulation of the Kv2.1 potassium channel by MinK and MiRP1. J Membr Biol 2009;228:1–14.
13. Zhang M, Jiang M, Tseng GN. MinK-related peptide 1 associates with Kv4.2 and modulates its gating function: potential role as beta subunit of cardiac transient outward channel? Circ Res 2001;88:1012–1019.
14. Delpon E, Cordeiro JM, Nunez L, et al. Functional effects of KCNE3 mutation and its role in the development of Brugada syndrome. Circ Arrhythm Electrophysiol 2008;1:209–218.
15. Roepke TK, Kontogeorgis A, Ovanez C, et al. Targeted deletion of *KCNE2* impairs ventricular repolarization via disruption of $I_{K,slow1}$ and $I_{to,f}$. FASEB J 2008;22:3648–3660.
16. Calloe K, Cordeiro JM, Di Diego JM, et al. A transient outward potassium current activator recapitulates the electrocardiographic manifestations of Brugada syndrome. Cardiovasc Res 2009;81:686–694.
17. Dixon JE, Shi W, Wang HS, et al. Role of the Kv4.3 K^+ channel in ventricular muscle. A molecular correlate for the transient outward current. Circ Res 1996;79:659–668.
18. Kääb S, Dixon J, Duc J, et al. Molecular basis of transient outward potassium current downregulation in human heart failure: a decrease in Kv4.3 mRNA correlates with a reduction in current density. Circulation 1998;98:1383–1393.
19. Benitah JP, Gomez AM, Bailly P, et al. Heterogeneity of the early outward current in ventricular cells isolated from normal and hypertrophied rat hearts. J Physiol 1993;469:111–138.
20. Singleton CB, Valenzuela SM, Walker BD, et al. Blockade by N-3 polyunsaturated fatty acid of the Kv4.3 current stably expressed in Chinese hamster ovary cells. Br J Pharmacol 1999;127:941–948.
21. Deschênes I, Tomaselli GF. Modulation of Kv4.3 current by accessory subunits. FEBS Lett 2002;528:183–188.
22. Wang S, Bondarenko VE, Qu Y, Morales MJ, Rasmusson RL, Strauss HC. Activation properties of Kv4.3 channels: time, voltage and $[K^+]_o$ dependence. J Physiol 2004;557:705–717.
23. An WF, Bowlby MR, Betty M, et al. Modulation of A-type potassium channels by a family of calcium sensors. Nature 2000;403:553–556.
24. Decher N, Uyguner O, Scherer CR, et al. hKChIP2b is a functional modifier of hKv4.3 potassium channels: cloning and expression of a short hKChIP2b splice variant. Cardiovasc Res 2001;52:255–264.
25. Radicke S, Cotella D, Graf EM, et al. Functional modulation of the transient outward current I_{to} by *KCNE* beta-subunits and regional distribution in human non-failing and failing hearts. Cardiovasc Res 2006;1:695–703.
26. Deschênes I, DiSilvestre D, Juang GJ, Wu RC, An WF, Tomaselli GF. Regulation of Kv4.3 current by KChIP2b splice variants: a component of native cardiac I_{to}? Circulation 2002;106:423–429.
27. Radicke R, Vaquero M, Caballero R, et al. Effects of MiRP1 and DPP6 β-subunits on the blockade induced by flecainide of Kv4.3/KChIP2 channels. Br J Pharmacol 2008;154:774–786.
28. Wettwer E, Amos GJ, Posival H, Ravens U. Transient outward current in human ventricular myocytes of subepicardial and subendocardial origin. Circ Res 1994; 75:473–482.
29. Patel SP, Campbell DL. Transient outward potassium current, "I_{to}," phenotypes in the mammalian left ventricle: underlying molecular, cellular and biophysical mechanisms. J Physiol 2005;569:7–39.
30. Antzelevitch C. Brugada syndrome. Pacing Clin Electrophysiol 2006;29:1130–1159.
31. Bezzina C, Veldkamp MW, van den Berg MP, et al. A single Na^+ channel mutation causing both long-QT and Brugada syndromes. Circ Res 1999;85: 1206–1213.
32. Van den Berg MP, Wilde AA, Viersma TJW, et al. Possible bradycardic mode of death and successful pacemaker treatment in a large family with features of long QT syndrome type 3 and Brugada syndrome. J Cardiovasc Electrophysiol 2001;12:630–636.

Long QT syndrome with compound mutations is associated with a more severe phenotype: A Japanese multicenter study

Hideki Itoh, MD, PhD,* Wataru Shimizu, MD, PhD,† Kenshi Hayashi, MD, PhD,‡ Kenichiro Yamagata, MD,† Tomoko Sakaguchi, MD, PhD,* Seiko Ohno, MD, PhD,§ Takeru Makiyama, MD, PhD,§ Masaharu Akao, MD, PhD,§ Tomohiko Ai, MD, PhD,¶ Takashi Noda, MD, PhD,† Aya Miyazaki, MD,‖ Yoshihiro Miyamoto, MD, PhD,** Masakazu Yamagishi, MD, PhD,‡ Shiro Kamakura, MD, PhD,† Minoru Horie, MD, PhD*

*From the *Department of Cardiovascular and Respiratory Medicine, Shiga University of Medical Science, Otsu, Japan, †Division of Arrhythmia and Electrophysiology, Department of Cardiovascular Medicine, National Cerebral and Cardiovascular Center, Suita, Japan, ‡Division of Cardiovascular Medicine, Kanazawa University Graduate School of Medical Science, Kanazawa, Japan, §Department of Cardiovascular Medicine, Kyoto University Graduate School of Medicine, Kyoto, Japan, ¶Texas Heart Institute/St. Luke's Episcopal Hospital, Houston, Texas, ‖Department of Pediatric Cardiology, National Cerebral and Cardiovascular Center, Suita, Japan, and **Laboratory of Molecular Genetics, National Cerebral and Cardiovascular Center, Suita, Japan.*

BACKGROUND: Long QT syndrome (LQTS) can be caused by mutations in the cardiac ion channels. Compound mutations occur at a frequency of 4% to 11% among genotyped LQTS cases.

OBJECTIVE: The purpose of this study was to determine the clinical characteristics and manner of onset of cardiac events in Japanese patients with LQTS and compound mutations.

METHODS: Six hundred three genotyped LQTS patients (310 probands and 293 family members) were divided into two groups: those with a single mutation (n = 568) and those with two mutations (n = 35). Clinical phenotypes were compared between the two groups.

RESULTS: Of 310 genotyped probands, 26 (8.4%) had two mutations in the same or different LQTS-related genes (compound mutations). Among the 603 LQTS patients, compound mutation carriers had significantly longer QTc interval (510 ± 56 ms vs 478 ± 53 ms, $P = .001$) and younger age at onset of cardiac events (10 ± 8 years vs 18 ± 16 years, $P = .043$) than did single mutation carriers. The incidence rate of cardiac events before age 40 years and use of beta-blocker therapy among compound mutation carriers also were different than in single mutation carriers. Subgroup analysis showed more cardiac events in LQTS type 1 (LQT1) and type 2 (LQT2) compound mutations compared to single LQT1 and LQT2 mutations.

CONCLUSION: Compound mutation carriers are associated with a more severe phenotype than single mutation carriers.

KEYWORDS Compound; Gene; Long QT syndrome; Mutation

ABBREVIATION QTS = long QT syndrome

(Heart Rhythm 2010;7:1411–1418)

Introduction

Congenital long QT syndrome (LQTS) is a heterogeneous disease characterized by prolonged ventricular repolarization and episodes of syncope and/or life-threatening cardiac arrhythmias, particularly polymorphic ventricular tachycardia.[1] Several disease-causing genes have been identified, including genes encoding cardiac ion channel-composing proteins, namely, *KCNQ1* (LQT1), *KCNH2* (LQT2), *SCN5A* (LQT3), *KCNE1* (LQT5), *KCNE2* (LQT6), *KCNJ2* (LQT7), and *CACNA1C* (LQT8), and genes encoding a family of versatile membrane adapters, namely, *ANK2* (LQT4), *CAV3* (LQT9), *SCN4B* (LQT10), *AKAPs* (LQT11), and *SNTA1* (LQT12).[2–5] Two modes of inheritance are involved in this syndrome, which exhibits both an autosomal dominant and an autosomal recessive pattern. The majority of LQTS cases are inherited in an autosomal dominant fashion. This pattern, which has been named as Romano-Ward syndrome,[6,7] can result from a single mutation in one

Drs. Shimizu, Makiyama, Akao, Miyazaki, Miyamoto, Yamagishi, and Horie were supported in part by a Health Sciences Research Grant (H18-Research on Human Genome-002) and a Research Grant for the Cardiovascular Diseases (21C-8) from the Ministry of Health, Labour and Welfare, Japan. Dr. Itoh was supported in part by a Grant-in-Aid for Young Scientists from the Ministry of Education, Culture and Technology. Dr. Horie was supported by the Uehara Memorial Foundation. Drs. Itoh and Shimizu contributed equally to this study. **Address reprint requests and correspondence:** Dr. Wataru Shimizu, Division of Arrhythmia and Electrophysiology, Department of Cardiovascular Medicine, National Cerebral and Cardiovascular Center, 5-7-1 Fujishiro-dai, Suita, Osaka 565-8565, Japan. E-mail address: wshimizu@hsp.ncvc.go.jp. (Received 7 February 2010; accepted June 3, 2010.)

1547-5271/$ -see front matter doi:10.1016/j.hrthm.2010.06.013

of the LQTS candidate genes. On the other hand, Jervell and Lange-Nielsen syndrome, which is inherited in an autosomal recessive fashion, is very rare,[8] affecting less than 1% of LQTS cases. It is caused by homozygous or compound heterozygous mutations of *KCNQ1* or *KCNE1*.[9,10]

Genetic analysis sometimes reveals two or more mutations in LQTS patients with clinical phenotypes of Romano-Ward syndrome. These compound mutations were shown to be associated with an increased arrhythmic risk.[11,12] However, most previous studies were conducted in Caucasian patients, and few systematic studies have involved Asian cohorts. In the present study, we analyzed the clinical characteristics of LQTS patients who were registered in a Japanese multicenter study. Analysis of the more 600 genotyped patients revealed that LQTS patients with compound mutations not only were common in Japan (8.4% among probands) but were associated with longer QTc and earlier onset of cardiac events. In patients who initially are diagnosed as LQT1 or LQT2, additional mutations may be present if patients have a more severe phenotype than expected; therefore, conducting a survey for major LQTS-related genes is critically important.

Methods

Patients and data collection

Major candidate genes were analyzed in 612 consecutive and unrelated probands with a suspected clinical diagnosis of congenital LQTS, who were referred to four centers in Japan (Shiga University of Medical Science, Otsu; Kyoto University Graduate School of Medicine, Kyoto; Kanazawa University Graduate School of Medical Science, Kanazawa; and National Cardiovascular Center, Suita) between June 1996 and January 2009. If gene mutations in LQTS-related genes were identified, further genetic analysis was conducted among family members as extensively as possible. All patients in the cohort were Japanese.

Genetic analysis

Informed consent was obtained from all individuals or their guardians according to standards established by the local institutional review boards. Genotypic and DNA sequence analyses of *KCNQ1, KCNH2, SCN5A, KCNE1,* and *KCNE2* were performed as described previously.[13] In addition, *KCNJ2* (Andersen syndrome [LQT7][14,15]) was analyzed in patients who had not only QT prolongation but also the clinical phenotype of Andersen syndrome, for example, periodic paralysis or dysmorphic features. Other candidate genes (e.g., ankyrin-B [LQT4], *CACNA1C* [Timothy syndrome, LQT8]) were not analyzed because mutations in these genes are extremely rare. Denaturing high-performance liquid chromatography was performed as described previously.[16] Abnormal conformers were amplified by polymerase chain reaction and sequenced using an ABI PRISM310 DNA sequencer (Perkin-Elmer Applied Biosystems, Wellesley, MA, USA). "Splicing error" mutations were defined as those that occurred within three bases of the splicing sites. When mutations were detected, 200 Japanese control subjects were checked and single nucleotide polymorphisms were excluded from the study. If mutations of these genes were detected in the probands, their family members were also analyzed and genotype–phenotype correlations confirmed. Mutation-negative controls were defined as family members without mutations detected in each proband. Nonsynonymous as well as synonymous single nucleotide polymorphisms were excluded with the assistance of data from previous reports[17–19] and from the National Center for Biotechnology Information database.

Clinical characterization

Baseline clinical data were recorded for each patient and included the following: age at diagnosis, age at first cardiac event, sex, cardiac events, family history of sudden cardiac death or LQTS members, ECG measurements, and therapeutic regimens administered. Schwartz scores also were calculated.[20,21] In the analysis of triggers of arrhythmic events, triggers were divided into four categories: exercise/swimming, emotional stress/arousal stress, sleep/rest, and other conditions.

ECG parameters measured at baseline included RR, QT_{end}, QT_{peak}, and $T_{peak\text{-}end}$ ($QT_{end\text{-}peak}$) intervals. The latter is thought to reflect transmural dispersion of ventricular repolarization.[22] Measurements were the mean of at least three beats measured in lead V_5 from the 12-lead ECG during stable sinus rhythm and corrected by the Bazett formula.[23] QT_{end} was manually measured as the time interval between QRS onset (Q) and the point at which the isoelectric line intersected a tangential line drawn at the maximal downslope of the positive T wave or the maximal

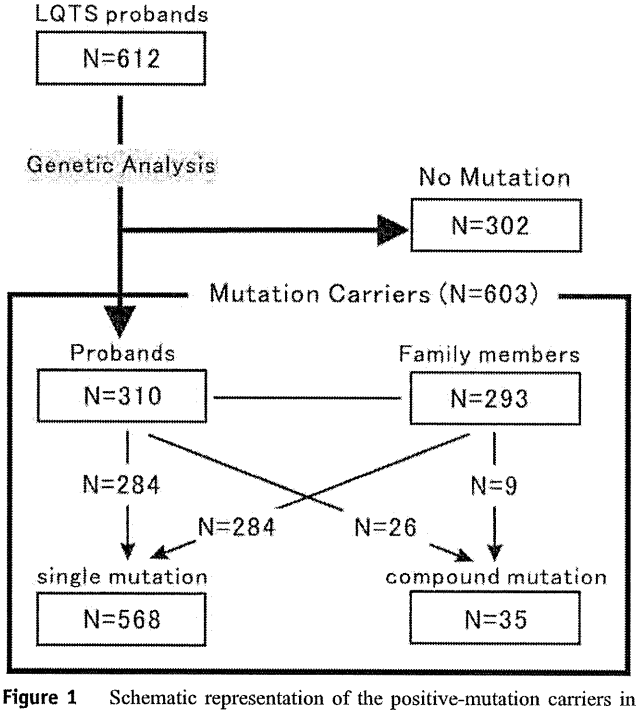

Figure 1 Schematic representation of the positive-mutation carriers in this study. LQTS = long QT syndrome.

Table 1 Overall data of patients with compound mutations

Research groups	Schwartz et al.	Westenkow et al.	Tester et al.	This study
Reported years	2003	2004	2005	2010
The corresponding number in the reference list	25	11	12	
Percentage of probands with compound mutations (probands with compound mutations/total probands) subtypes	4.6% (6/130)	5.2% (9/172*)	10.8% (29/269)	8.4% (26/310)
LQT1	7 (58%)	14 (35%)	30 (52%)	18 (35%)
LQT2	2 (17%)	10 (25%)	15 (26%)	17 (33%)
LQT3	3 (25%)	2 (5%)	13 (22%)	14 (27%)
LQT5-D85N	0 (0%)	10 (25%)	0 (0%)	0 (0%)
vs. single mutation carriers				
QTc interval	NA	prolonged	not significant	prolonged
Cardiac events	NA	frequent	not significant	not significant
Age of onset	NA	NA	younger onset	younger onset

*This table excluded probands with single nucleotide polymorphisms (SNP), NA = not available.

upslope of the negative T wave (QT_{end}). $QT_{end\text{-}peak}$ then was obtained by calculating as QT_{end} minus QT_{peak}.

Statistical analysis

All analyses were performed using the SPSS 16.0 statistical package (SPSS, Inc., Chicago, IL. USA). Data are expressed as mean ± SD. $P < 0.05$ was considered significant. Univariate comparison of parameters between groups was performed by an unpaired t-test. Differences in incidence between groups were analyzed by Chi-square test or Fisher exact probability test. The cumulative probability of a first cardiac event (syncope, torsades de pointes, ventricular fibrillation, cardiac arrest, or sudden death) occurring before age 40 years and before beta-blocker therapy or after beta-blocker therapy was determined by means of the life-table method of Kaplan-Meier, and results were compared using log rank test.[24]

Results

Genetic characteristics of mutations associated with single and compound mutations

Genetic analysis revealed gene mutations in 310 (51%) of 612 probands. The study enrolled 603 genotyped LQTS patients consisting of 310 genotyped probands and their 293 genotyped family members. A flowchart of the genetic diagnosis of the study population is shown in Figure 1.

Of the 310 genotyped probands, 26 (8.4%) had compound mutations. This rate is comparable to the rates in previous reports of Caucasian patients (Table 1). The 26 probands all had two mutations in the LQTS-related genes we examined. These 52 mutations in 26 probands consisted of 45 missense mutations, 4 frameshift mutations, 2 splice-site mutations, and 1 nonsense mutation (see Online Supplemental Data 1). The mutation types of the 284 single mutation carriers were 210 missense mutations, 34 frameshift mutations, 18 splicesite mutations, 12 deletions, 9 nonsense mutations, and 1 insertion mutation (see Online Supplemental Data 2). Therefore, the mutation types were similar between the two groups (Figure 2).

Among the 293 genotyped family members, there were 284 single mutation carriers and 9 compound mutation carriers. In total, 568 patients with a single mutation (284 probands and 284 family members) consisted of 256 with LQT1, 248 with LQT2, 62 with LQT3, and 2 with LQT5. Thirty-five compound mutation carriers (26 probands and 9 family members) consisted of 9 with LQT2 and LQT3, 7 with LQT1 and LQT2, 6 with LQT1 and LQT3, 4 with double LQT1, 3 with double LQT2 mutations, 2 with LQT1 and LQT7, 2 with LQT2 and LQT7, 1 with double LQT3, and 1 with LQT1 and LQT6.

Families associated with compound mutations

In the analysis of family members associated with compound mutations, 28 single heterozygous mutation carriers and 4 obligate single mutation carriers were identified from 9 families, and single mutation carriers had milder clinical phenotypes than compound mutation carriers (Figure 3). Only 2 (6%) of the 32 single mutation carriers had syncope but no torsades de pointes, an incidence lower than that in compound mutation carriers (54% [19/35] patients, $P < .001$). For single heterozygous mutation carriers in compound mutation families, average QTc interval was 442 ± 30 ms, which was longer than that of the 15 mutation-negative controls (408 ± 28 ms, $P = .001$) but significantly shorter than that of compound mutation carriers (510 ± 56 ms, $P < .001$).

Early onset of cardiac events and more severe QT prolongation was observed in patients with compound mutations

Table 2 compares the clinical characteristics of 35 LQTS patients with compound mutation and 568 LQTS patients with a single mutation. The female-to-male ratio was similar between the two groups. However, the incidence of family members associated with double-hit patients was significantly smaller than that with a single mutation (26% vs 50%, $P = .005$). In the ECG analysis of 496 patients with available information, corrected QT interval was significantly longer in compound mutation carriers than in single mutation carriers (510 ± 56 ms vs 478 ± 53 ms, respectively, $P = .001$), whereas other ECG findings, R-R interval, corrected QT_{peak}, corrected $QT_{peak\text{-}end}$, and rates of

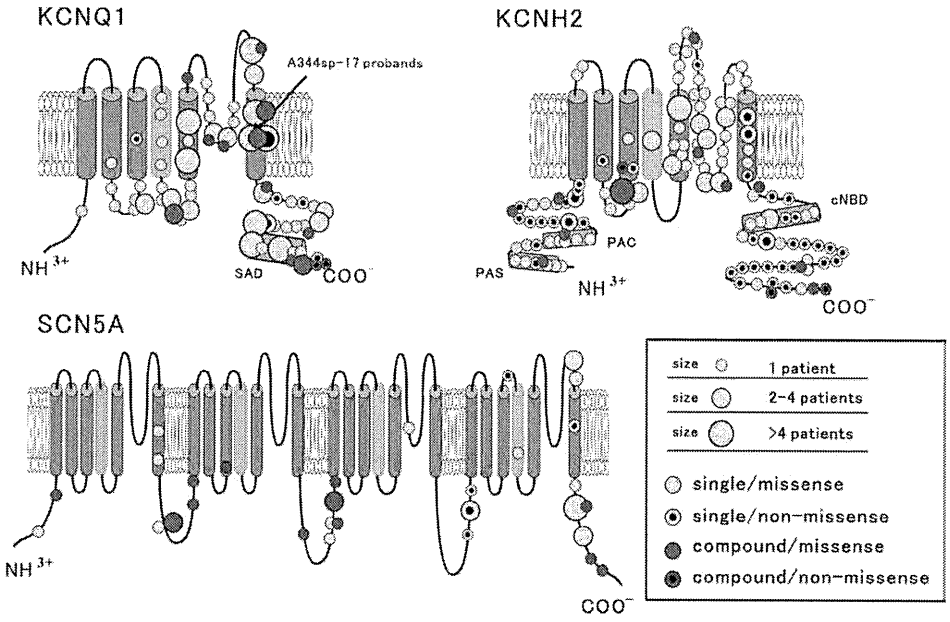

Figure 2 Conventional transmembrane topology of all mutations in the probands.

notched T wave and T-wave alternans were not different between the two groups. The frequency of patients with a normal QTc interval <440 ms was similar between the two groups, whereas the frequency of double-hit patients with QTc intervals >500 ms was significantly higher than in those with a single mutation (66% vs 26%, $P < .001$). Schwartz scores in the compound mutation group and the rate of patients with a score ≥4 were higher than those in the single mutation group (Schwartz score: 4.3 ± 2.1 vs 3.4 ± 1.9 points, $P = .017$; rates of Schwartz score ≥4 points: 70% vs 47%, $P = .026$). A significantly higher number of patients with compound mutations received beta-blocker therapy than did those with a single mutation (56% vs 33%, $P = .006$).

In the analysis of "all age groups," the frequency of cardiac events was similar between compound and single mutation groups, whereas age at first cardiac event was significantly lower in the compound mutation group (10 ± 8 years vs 18 ± 16 years, $P = .043$). For the occurrence of syncope or torsades de pointes before age 40 years, compound mutation carriers had significantly more events than did single mutation carriers (54% vs 37%, $P = .043$). The occurrence of cardiac arrest or ventricular fibrillation was similar between the two groups for patients before age 40 years. In 561 patients with available information on age at first cardiac events, Kaplan-Meier analysis showed that the cumulative rate of survival without a cardiac event before age 40 years and use of beta-blocker therapy differed significantly between compound and single mutation carriers ($P = .004$ by log rank test; Figure 4A) and between compound mutation carriers and each subgroup of single mutation carriers ($P = .004$ vs LQT1, $P = .018$ vs LQT2, $P = .001$ vs LQT3, by log rank test; Figure 4B). In the analysis of matched subtypes between single and compound mutation carriers, patients with additional mutations in an LQTS subtype had a significantly poorer prognosis than LQT1 alone ($P = .001$; Figure 5) and LQT2 alone ($P = .035$) but not LQT3 alone ($P = .06$).

Discussion

In this multicenter study, the major findings were as follows. (1) LQTS-associated compound mutations in the Japanese population were as common as previously reported in studies of Caucasian patient cohorts. (2) Patients with compound mutations displayed longer QTc and earlier onset of cardiac events. (3) Patients with compound mutations had more cardiac events before age 40 years and more beta-blocker therapy. (4) Subgroup analysis showed more cardiac events in LQT1 and LQT2 compound mutations compared to single LQT1 and LQT2 mutations.

Twenty-six probands (8.4% of genotyped LQTS) were found to have two variants in genes encoding ion channels *(KCNQ1, KCNH2, SCN5A, KCNE1, KCNE2,* or *KCNJ2)*. This incidence rate is in general agreement with other studies that reported a prevalence of compound or multiple mutations of 5% to 11% of genotyped LQTS (Table 1).[11,18,25]

Table 1 summarizes the genetic and clinical characteristics of patients enrolled in previous studies and compares them with the characteristics of patients enrolled in the present study. Sanguinetti and colleagues reported that patients with compound mutations not only had longer QT intervals than single mutation carriers but also had more frequent cardiac events.[11] However, Ackerman and colleagues demonstrated that, although compound mutation carriers were diagnosed at a younger age than single mutation carriers, they did not have significantly longer QT intervals.[12] The difference between these results might be explained by half of the 20 compound probands in the cohort of Sanguinetti et al possessing the common *KCNE1-*

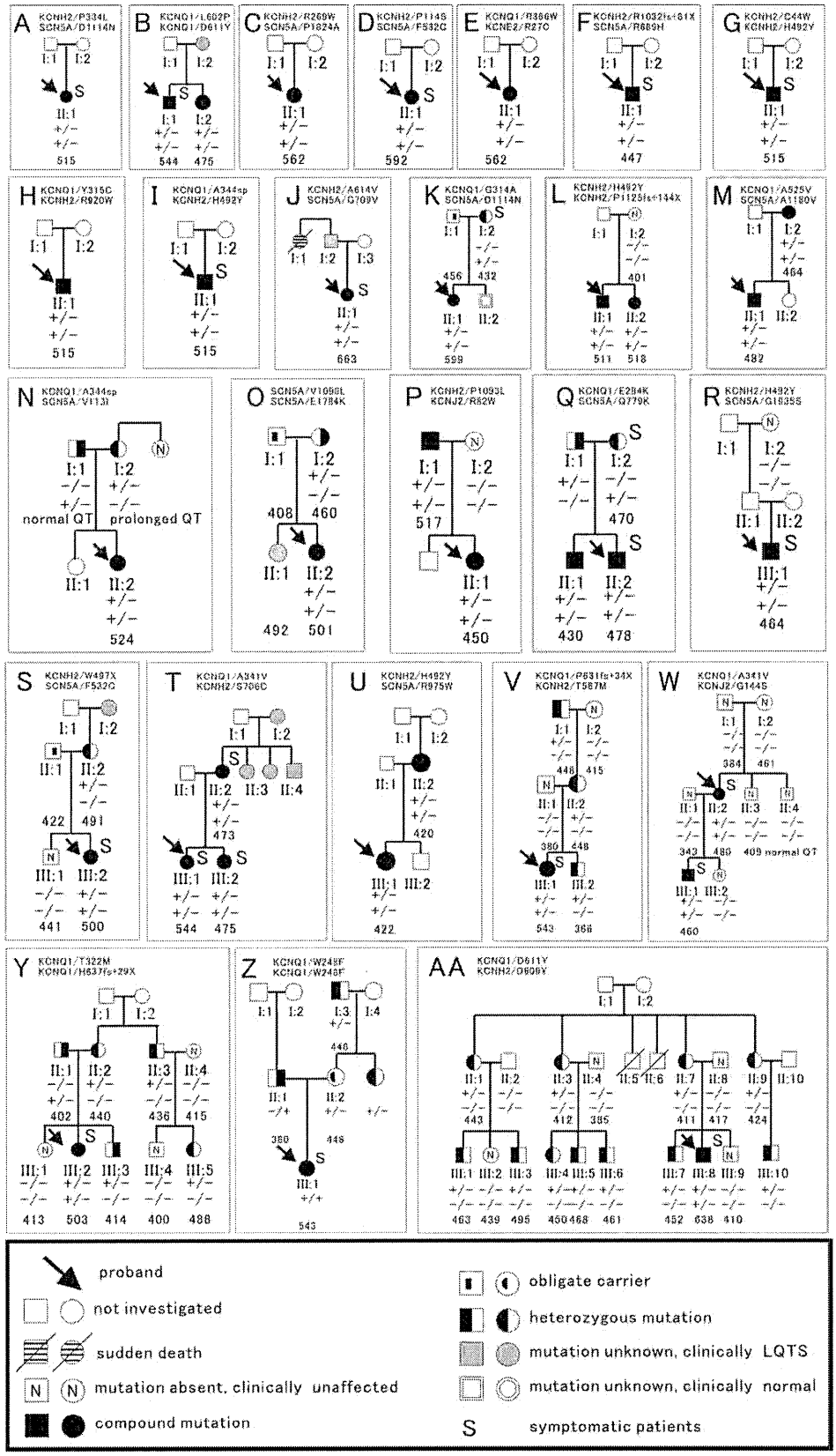

Figure 3 Pedigrees of the families associated with compound mutation probands.

Table 2 Clinical characteristics of LQTS patients with gene mutations

	Compound mutations (N=35)	Single mutations (N=568)	p value
Demographic			
Age at diagnosis (yrs)	19 ± 14 [15, 9–27]	28 ± 19 [22, 12–42]	0.001
Female gender	23 (66%)	330 (58%)	0.394
Proband	26 (74%)	284 (50%)	0.005
Family members	9 (26%)	284 (50%)	0.005
Cardiac events			
cardiac events in all age groups			
Age at first cardiac event (yrs)	10 ± 8 [11, 3.5–13.5]	18 ± 16 [12, 7–19]	0.043
syncope	19 (54%)	235 (41%)	0.161
TdP	10 (29%)	102 (18%)	0.136
cardiac arrest or VF	3 (9%)	44 (8%)	0.748
sudden death	0 (0%)	4 (1%)	1.000
cardiac events before 40 yrs			
syncope or TdP	19 (54%)	205 (37%)	0.043
cardiac arrest or VF	3 (9%)	37 (7%)	0.500
ECG measurements			
RR interval (ms)	866 ± 210	914 ± 174	0.252
corrected QT (ms)	510 ± 56	478 ± 53	0.001
corrected QT >500 ms (%)	23 (66%)	122 (26%)	<0.001
corrected QT <440 ms (%)	3 (9%)	91 (20%)	0.351
corrected QT peak (ms)	385 ± 70	384 ± 50	0.906
corrected QT peak-end (ms)	121 ± 73	95 ± 41	0.081
notched T wave	11 (31%)	200 (37%)	0.540
T-wave alternans	0 (0%)	30 (5%)	0.246
Diagnosis			
Schwartz score	4.2 ± 2.1	3.4 ± 1.9	0.017
Schwartz score ≧4	21 (70%)	219 (47%)	0.026
Therapy			
β-blocker	10 (56%)	175 (33%)	0.006
class Ib antiarrhythmic drugs	3 (9%)	53 (10%)	1.000
pacemaker	1 (3%)	15 (3%)	1.000
sympathectomy	1 (3%)	3 (1%)	0.218
defibrillator	1 (3%)	32 (6%)	0.712

TdP = torsades de pointes, VF = ventricular fibrillation, NS = not significant, corrected QT = QT interval corrected for heart rate with Bazett formula [A, B], A = median, B–C = first interquartile range–third interquartile range.

D85N polymorphism as the "second hit" (Table 1).[11,26] In all age groups of this study, the incidence of cardiac events, such as torsades de pointes or syncope, was similar between single and compound mutation carriers; however, the clinical phenotypes of those with compound mutations before 40 years of age were more serious than in those with a single mutation (Table 2). Thus, phenotypes with compound mutations appear to be more serious than single mutation carriers, regardless of race.

Beta-blocker therapy is first-line treatment for the prevention of cardiac events in LQTS. Beta-blockers have been shown to significantly reduce cardiac events in LQTS patients, especially LQT1 type.[27–29] However, patients with LQT2 or LQT3 have been reported to be less responsive to beta-blocker therapy[27,30] and may require additional therapy, such as pacemaker implantation for LQT2 or a Class Ib antiarrhythmic drug for LQT3. It may be recommended that patients with compound mutations receive additional individual therapy based on their LQTS subtype, for example, the combination of beta-blocker and Class Ib antiarrhythmic drugs for patients with LQT1 and LQT3. In patients who were first diagnosed as LQT1, Kobori et al[31] reported that additional mutations in different LQTS-related genes influenced phenotype severity and reduced beta-blocker effectiveness. Previous reports showed that approximately 20% of LQT1 patients were resistant to beta-blocker therapy. Additional or "latent" mutations may be present in these patients, and conducting a survey for major all LQTS-related genes, even after a possible mutation is identified, is critically important.

Family study analyses are of enormous importance because single mutation carriers in this study tended to have mild phenotypes. Most of the single mutation carriers in families of compound probands remained asymptomatic. However, double hits of these "latent" gene carriers could cause more serious phenotypes.[32,33] Jervell and Lange-Nielsen syndrome is a well-documented LQTS phenotype with an autosomal recessive pattern. The loss of function of I_{Ks} on both alleles generally causes not only more severe clinical phenotypes but also deafness.[9,10] In our study, two of three probands with double *KCNQ1* mutations had no deafness. We speculate that these mutations would functionally cause mild changes without complete loss of I_{Ks}. Westenskow et al[11] reported the molecular mechanism of

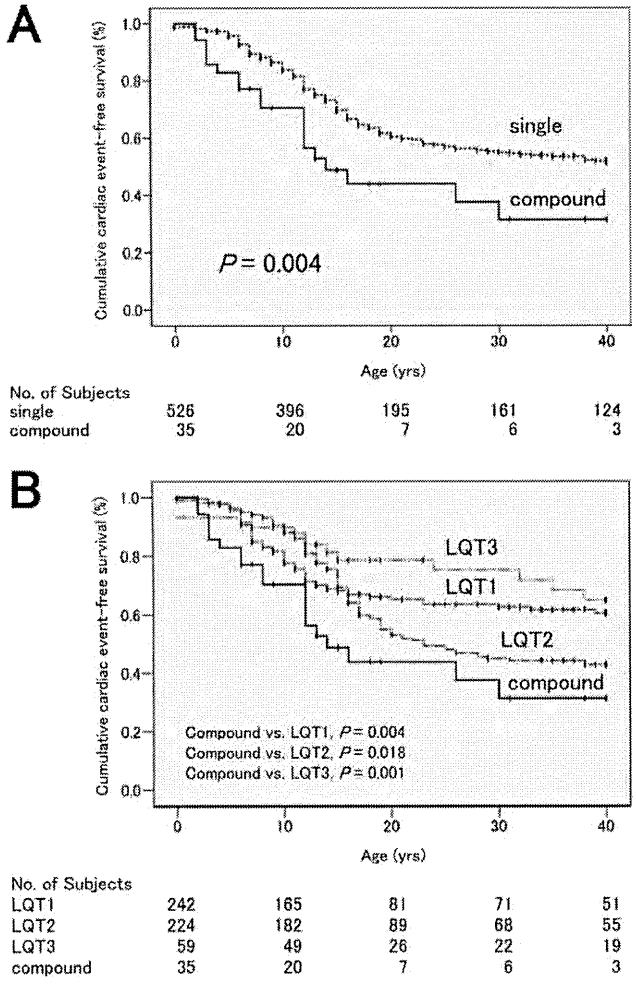

Figure 4 Kaplan-Meier cumulative probability of cardiac event-free survival from birth to age 40 years and before therapy. **A:** Comparison between patients with a single mutation and compound mutations. **B:** Comparison among patients with long QT syndrome type 1 (LQT1), type 2 (LQT2), type 3 (LQT3), and compound mutations.

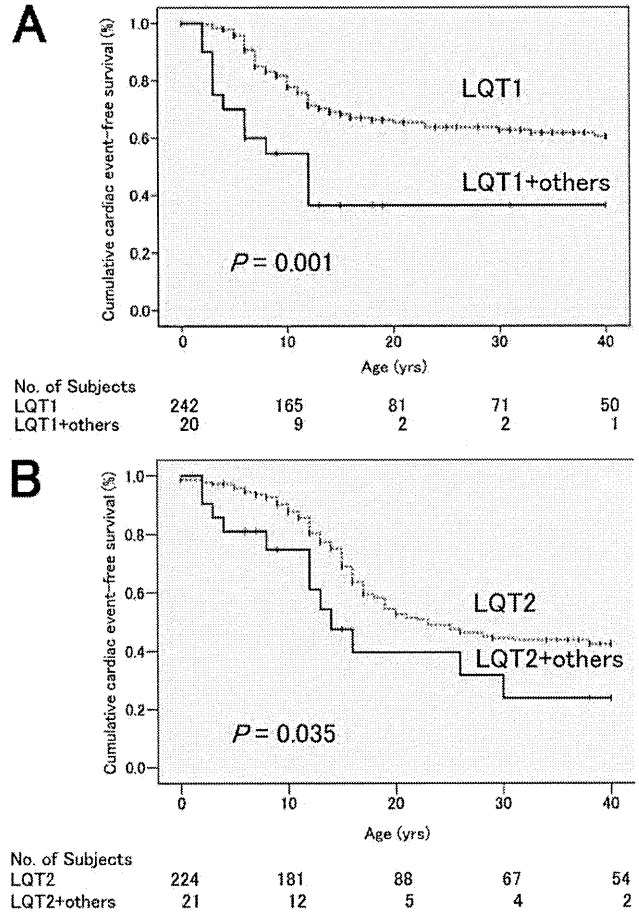

Figure 5 Kaplan-Meier cumulative probability of cardiac event-free survival from birth to 40 years of age and before therapy. **A:** Comparison between patients with long QT type 1 (LQT1_ subtype and compound mutation carriers with LQT1 plus other mutations. **B:** Comparison between patients with long QT syndrome type 2 (LQT2) and those with LQT2 plus other mutations.

increased risk through compound mutations using heterologous expressions in *Xenopus* oocytes. When wild-type and variant subunits were coexpressed in appropriate ratios to mimic the genotype of the probands with mutations, the reduction in current density was equivalent to the additive effects of the single mutations. Coexpression of two mutant subunits caused a significant but incomplete reduction. Thus, either compound mutation seems to be associated with mild functional damage. It is necessary to have "double hits" of these mild mutations in order to produce symptoms.

Study limitations

This study has several limitations. First, six major LQTS candidate genes were examined, but not for minor genes encoding a family of versatile membrane adapters. However, excluding these minor genes from our investigations would not have affected the overall study results, largely because the incidence of these minor gene mutations reportedly is ≤1%. Second, analysis of single mutation carriers in compound mutation families is dominated by their presence in only 35% (9/26) of families. Therefore, there might be a statistical bias due to a mutation-specific effect. Third, Kapa et al[19] reported the need for further studies on whether regions such as the interdomain linker of *SCN5A* could affect the clinical phenotypes of LQTS. In this study, we were able to distinguish mutations from these "genetic noises," especially in the *SCN5A* gene.

Acknowledgment

We thank Professor Pascale Guicheney (INSERM, U956, Group Hospitalier Pitié-Salpêtrière, Paris) for advice and review of the manuscript.

Appendix

Supplementary data

Supplementary data associated with this article can be found, in the online version, at doi:10.1016/j.hrthm.2010.06.013.

References

1. Moss AJ, Zareba W. Long QT syndrome: therapeutic considerations. In: Zipes DP, Jalife J, editors. Cardiac Electrophysiology: From Cell to Bedside. Philadelphia: WB Saunders, 2004:660–667.